1 MW J-PARC RCS BEAM OPERATION AND FURTHER BEYOND

H. Hotchi[1†], H. Harada[2], N. Hayashi[2], M. Kinsho[2], K. Okabe[2], P.K. Saha[2], Y. Shobuda[2],
F. Tamura[2], K. Yamamoto[2], M. Yamamoto[2] and M. Yoshimoto[2]
Accelerator Division, J-PARC Center, [1]KEK/[2]JAEA, Tokai, Ibaraki, Japan

Abstract

The J-PARC 3-GeV rapid cycling synchrotron has achieved a 1-MW beam operation with considerably low fractional beam loss of a couple of 10^{-3}. Following this successful achievement, we have recently conducted further high-intensity beam tests toward a higher beam power beyond 1 MW. This paper reviews our continuous efforts for beam loss mitigation including the recent result of a 1.5-MW-equivalent high-intensity beam test.

INTRODUCTION

The J-PARC 3-GeV rapid cycling synchrotron (RCS) is a world leading high-power pulsed proton driver, which has the goal of achieving a 1-MW beam power [1, 2]. A 400-MeV negative hydrogen ion (H^-) beam from the injector linac is delivered to the RCS injection point, where it is multiturn charge-exchange injected through a carbon foil over a period of 0.5 ms (307 turns). The RCS accelerates the injected protons up to 3 GeV with a repetition rate of 25 Hz. Most of the RCS beam pulses are delivered to the materials and life science experimental facility (MLF), while only four pulses every several seconds (2.48 s or 5.2 s) are injected to the main ring (MR) by switching the beam destination pulse by pulse.

Figure 1 shows the history of the RCS beam power. In 2015, the beam power reached 500 kW. But it caused premature failures of the neutron production target two times in a row as shown by white arrows in Fig. 1, so that the beam power was reduced to 150–200 kW to prioritize availability for users. In 2017, a new improved target was installed. Since then, the beam power has been stepped up again while carefully monitoring the durability of the target. It now reaches 740 kW. If there are no unexpected troubles with the target from now on, the routine beam power will reach nearly 1 MW in two years.

Thus, we are still in the course of gradually increasing the beam power to 1 MW, but the accelerator itself has already well established a 1-MW beam operation. The most important issues in realizing such a MW-class high-power beam operation are controlling and minimizing beam loss, which are essential for sustainable beam operation that allows hands-on maintenance [3].

In high-power machines such as the RCS, there exist many factors causing beam loss, such as space charge, lattice imperfections and foil scattering. Besides, beam loss generally occurs through a complex mechanism involving several factors. In the RCS, numerical simulations have played a vital role in solving beam loss issues in combination with actual beam experiments; various ideas for beam loss mitigation were proposed with the

help of the numerical simulations, and verified by experiments. As a result of such continuous efforts including several hardware improvements, we have recently accomplished a 1-MW beam acceleration with considerably low fractional beam loss of several 10^{-3} [4, 5].

This paper reviews our approaches to beam loss issues that we faced in the course of beam power ramp-up. Our recent efforts to further beam power ramp-up beyond 1 MW are also presented.
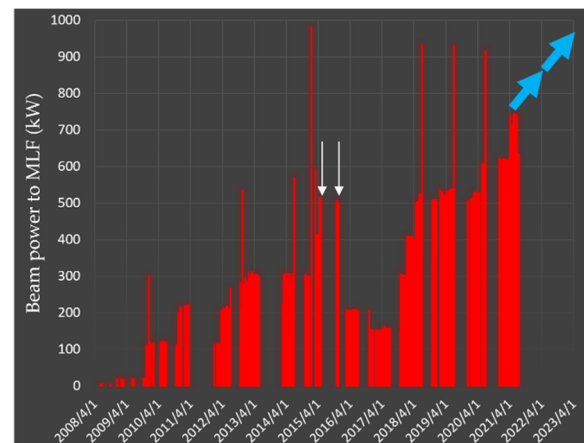

Figure 1: History of the RCS beam power.

REVIEW OF BEAM TUNING FOR BEAM LOSS MITIGATION

Beam Loss Mitigation by Injection Painting

In high-intensity proton synchrotrons, space charge in the low-energy region is one of the most crucial sources of beam loss. To mitigate this, the RCS adopts transverse and longitudinal injection painting.

In transverse injection painting [6], the phase space offsets between the centroid of the injection beam and the ring closed orbit are varied during multi-turn injection. By this way, the injection beam is uniformly distributed over a required phase-space area. On the other hand, in longitudinal injection painting [7, 8], a momentum offset to the rf bucket is introduced during multi-turn injection. In this way, a uniform bunch distribution is formed through emittance dilution by a large synchrotron motion excited by the momentum offset. In addition, the second harmonic rf and its phase sweep are introduced, which enable further bunch distribution control through a dynamical change of the rf bucket potential. By this way, the charge density peak in the longitudinal direction is effectively reduced.

Figure 2 shows the beam survival rates measured without and with the injection painting. In the case with no

_____

† email address hideaki.hotchi@j-parc.jp

DEVELOPMENT OF AN INJECTION-PAINTED SELF-CONSISTENT BEAM IN THE SPALLATION NEUTRON SOURCE RING

A. Hoover, University of Tennessee, Knoxville, U.S.A.

N. J. Evans*, T. Gorlov, J. Holmes, Oak Ridge National Laboratory, Oak Ridge, U.S.A.

Abstract

A self-consistent beam maintains linear space charge forces under any linear transport, even with the inclusion of space charge in the dynamics. Simulation indicates that it is possible to approximate certain self-consistent distributions in a ring with the use of phase space painting. We focus on the so-called Danilov distribution, which is a uniform density, rotating, elliptical distribution in the transverse plane and a coasting beam in the longitudinal plane. Painting the beam requires measurement and control of the orbit at the injection point, and measuring the beam requires reconstruction of the four-dimensional (4D) transverse phase space. We discuss efforts to meet these requirements in the Spallation Neutron Source (SNS) ring.

INTRODUCTION

We define a self-consistent beam as one that maintains linear space charge forces under any linear transport, even with the inclusion of space charge in the dynamics. Several desirable properties stem from the linearity of the space charge force: the emittance is conserved, the space charge tune shift is minimized, and the space charge tune spread is eliminated. An ongoing project is to determine whether a self-consistent beam can be approximated in reality.

Various self-consistent distributions were derived in [1]; of particular interest for our purposes is the so-called Danilov distribution, which is a uniform density ellipse in the transverse plane and a coasting beam in the longitudinal plane. Particles in the distribution occupy elliptical modes so that the four-dimensional (4D) transverse emittance vanishes. Equivalently, one of the intrinsic emittances $\varepsilon_{1,2}$ vanishes depending on the sign of the angular momentum [2]. The intrinsic emittances are conserved even with space charge, but the apparent emittances $\varepsilon_{x,y}$ are not [3].

In the linear approximation, it is possible to create an approximate Danilov distribution in a circular machine using phase space painting. This can be done by moving the injection coordinates along an eigenvector of the ring transfer matrix with square root time-dependence. In other words,

$$\mathbf{x}(t) = \sqrt{2J}\, Re\left\{\mathbf{v}e^{-i\mu}\right\}\sqrt{t},\tag{1}$$

where $\mathbf{x} = (x, x', y, y')$ is the phase space location of the injection beam in the frame of the circulating beam, J is an amplitude, μ is a phase, $\mathbf{v}$ is an eigenvector of the ring transfer matrix, and t is a time variable normalized to the range [0, 1]. We call this *elliptical painting*. The turn-by-turn projection of the eigenvector onto any 2D subspace
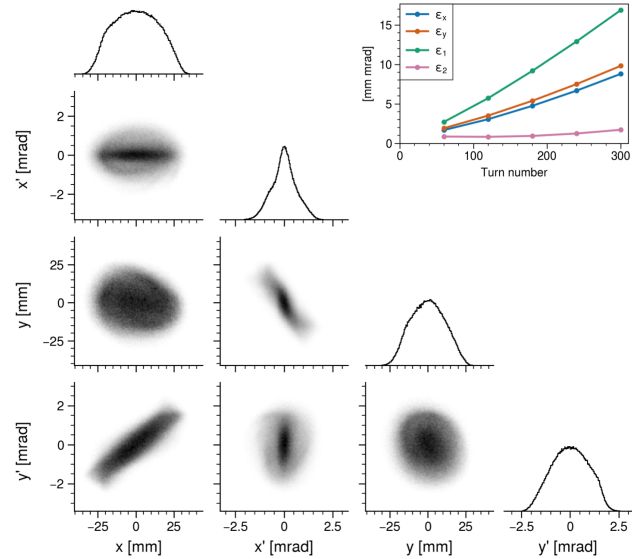

Figure 1: ORBIT simulation of elliptical painting in the SNS ring. Bottom left: 2D projections of the final 4D phase space distribution. Top right: emittance growth during injection.

of the 4D phase space will trace an ellipse, and the square root time-dependence ensures the uniform density of the projected distributions at all times. Since the particles lie along an eigenvector, the intrinsic emittance associated with the other eigenvector will be zero. We note that performing this method in an uncoupled lattice results in a flat beam ($\varepsilon_x = 0$ or $\varepsilon_y = 0$) unless the horizontal and vertical tunes are equal.

Simulations suggest that the various conditions required for elliptical painting to produce a self-consistent beam will approximately hold in the Spallation Neutron Source (SNS) [4]. Figure 1 shows the results of one such simulation. The core of the final 1D projections resemble those of ideal elliptical projections, and it can also be seen from the linear emittance growth and constant/small ε_2 that the beam remains reasonably close to a Danilov distribution during injection.

Several steps were necessary to achieve this simulated result. First, the painting path was chosen to follow a line in the x-y' plane. Deviation from this path was found to increase beam losses due to machine specifics. Additional motivation for x-y' painting comes from study of the beam envelope equations in [3]. The beam tilts throughout the ring, but the matched solution with space charge is upright at locations where $\alpha \approx 0$ such as the injection point. A tilted beam at

FIRST EXPERIENCE OF CRYSTAL COLLIMATORS DURING LHC SPECIAL RUNS AND PLANS FOR THE FUTURE*

M. D'Andrea[1,2†], V. Avati[1,3], R. Bruce[1], M. Butcher[1], M. Di Castro[1], M. Deile[1], B. Dziedzic[4],
H. Garcia Morales[1,5‡], Y. Gavrikov[1,6], K. Hiller[7], S. Jakobsen[1], J. Kašpar[1,8], K. Korcyl[4],
I. Lamas Garcia[1], A. Masi[1], A. Mereghetti[1§], D. Mirarchi[1,9], S. Redaelli[1], B. Salvachua Ferrando[1],
P. Serrano Galvez[1], M. Solfaroli Camillocci[1], N. Turini[10]

[1]CERN, European Organization for Nuclear Research, Geneva, Switzerland
[2]Università degli Studi di Padova, Padova, Italy
[3]AGH University of Science and Technology, Kraków, Poland
[4]Institute of Nuclear Physics, Polish Academy of Sciences, Kraków, Poland
[5]Royal Holloway University of London, Egham Hill, Egham, United Kingdom
[6]Petersburg Nuclear Physics Institute, NRC "Kurchatov Institute", Gatchina, Russia
[7]Deutsches Elektronen-Synchrotron, Hamburg, Germany
[8]Institute of Physics of the Czech Academy of Sciences, Prague, Czech Republic
[9]The University of Manchester, Manchester, United Kingdom
[10]Università degli Studi di Siena and Gruppo Collegato INFN di Siena, Siena, Italy

Abstract

Bent crystals can deflect charged particles by trapping them within the potential well generated by neighboring crystalline planes and forcing them to follow the curvature of the crystal itself. This property has been extensively studied over the past decade at the CERN accelerator complex, as well as in other laboratories, for a variety of applications, ranging from beam collimation to beam extraction and in-beam fixed target experiments. In 2018, crystal collimators were operationally used for the first time at the Large Hadron Collider (LHC) during a special high-β^* physics run with low-intensity proton beams, with the specific goal of reducing detector background and achieving faster beam halo removal. This paper describes the preparatory studies carried out by means of simulations, the main outcomes of the special physics run and plans for future uses of this innovative collimation scheme, including the deployment of crystal collimation for the High-Luminosity LHC upgrade.

INTRODUCTION

The CERN Large Hadron Collider (LHC) is routinely used to accelerate and collide high-intensity proton beams [1]. Throughout Run 2 (2015-2018), it was operated at a top energy of 6.5 TeV, with typical beam populations of a few 10^{14} protons per beam. In addition to the high-intensity, high-energy operation, special runs with dedicated machine and beam configurations were also performed in order to achieve specific experimental conditions.

In October 2018, one of the aforementioned special runs was carried out at the injection energy of 450 GeV, using low-intensity beams (up to about $6 \cdot 10^{11}$ protons per beam)

and a special optics with a β^* (i.e. the optical function at the Interaction Points, IPs) larger than in normal operation. This special run was requested by the forward physics community to measure the proton-proton elastic cross section and extrapolate its nuclear part towards low values of momentum transfer [2]. Dedicated detectors housed in movable Roman Pots (XRPs) [3] are transversely placed very close to the circulating beams in order to intercept particles scattered at small angles as result of collisions with low momentum transfer at the IP. Two sets of XRP stations are installed downstream of IP1 and IP5, and are operated by the ATLAS (ALFA) [4] and TOTEM [5] collaborations respectively. Only the vertical two-sided stations, whose layout is schematically illustrated in Fig. 1, were used for this run.
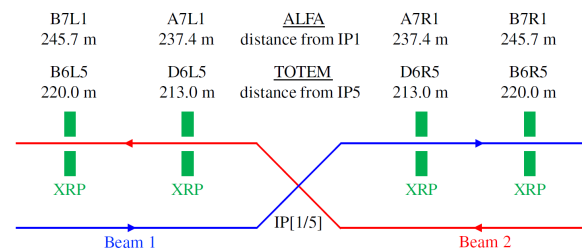

B7L1	A7L1	ALFA	A7R1	B7R1
245.7 m	237.4 m	distance from IP1	237.4 m	245.7 m
B6L5	D6L5	TOTEM	D6R5	B6R5
220.0 m	213.0 m	distance from IP5	213.0 m	220.0 m

Figure 1: Illustrative layout of the vertical ALFA and TOTEM XRPs stations around IP1 and IP5 [6].

The setup of this run posed several challenges from the accelerator physics point of view, requiring the design of dedicated beam optics [7] and collimation settings [8]. While machine protection requirements were relaxed thanks to the low stored beam energy of about 40 kJ (with respect to the stored energy of 350 MJ in nominal operation), the background induced at the detectors would have been intolerable without a dedicated halo collimation system. The feasibility of tight collimator settings necessary to position the XRPs as close as possible to the beam was identified as a major concern for the success of the run. In the standard LHC col-

---

IMPROVEMENT OF CAPTURE RATIO FOR AN X-BAND LINAC BASED ON MULTI-OBJECTIVE GENETIC ALGORITHM*

Junyang Li, Tongning Hu†, Jun Yang, Bingqian Zeng, Hongjie Xu, Lanxin Nie

Huazhong University of Science and Technology, Wuhan, China

Abstract

Electron linear accelerators with an energy of ~MeV are widely required in industrial applications. Whereas miniaturized accelerators, especially those working at X-band, attract more and more attention due to their compact structures and high gradients. Since the performance of a traveling wave (TW) accelerator is determined by its structures, considerable efforts must be made for structure optimization involving numerous and complex parameters. In this context, functional key parameters are obtained through deep analysis for structure and particle motion characteristics of the TW accelerator, then a multi-objective genetic algorithm (MOGA) is successfully applied to acquire an optimized phase velocity distribution which can contribute to achieving a high capture ratio and a low energy spread. Finally, a low-energy X-band TW tube used for rubber vulcanization is taken as an example to verify the reliability of the algorithm under a single-particle model. The capture ratio is 91.2%, while the energy spread is 5.19%, and the average energy is 3.1MeV.

INTRODUCTION

Electron beams with energy of ~MeV have been widely applied in life and materials sciences, industrial radiography, wastewater treatment, non-destructive testing, and other fields [1-4]. In recent years, Chiang Mai University in Thailand has researched applying electron beam of ~MeV to rubber vulcanization. The research on vulcanization of rubber was carried out by Chiang Mai University in Thailand Considering the difference in material thickness and density, the beam energy is generally 1-4 MeV [5-7].

RF linac is a commonly used scheme to obtain electron beam of ~MeV, but the traditional S-band accelerator structure and supporting power sources are relatively large, which is not suitable for cargo inspection and other occasions requiring accelerator miniaturization [8]. In contrast, the X-band increases the operating frequency by about three times, which has the advantages of a high acceleration gradient and compact structure. At present, many accelerator laboratories have developed X-band accelerators [9-13].

In the design of phase velocity for the TW tubes, it is often necessary to try repeatedly according to engineering experience, which is time-consuming and difficult to gain the optimal performance parameters. In 2002 Deb proposed nondominated sorting genetic algorithm II (NSGA-II), which has good convergence and diversity in solving multi-objective problems [14]. Based on NSGA-II, many

accelerator-related optimization problems have been completed, such as beam matching and beam transport in the low and medium energy section of a modern hadron linac [15], undulator taper profile and focusing scheme of a seeded free electron laser (FEL) [16], the optimal working point of a linac driver for a seeded FEL [17], the nonlinear lattice and dynamic aperture for the high energy photon source storage ring [18,19].

In consequence, it is of engineering significance to optimize the phase velocity of low-energy X-band TW tubes by using the multi-objective genetic algorithm. After introducing the mathematical and physical model of TW acceleration structure, NSGA-II is used to obtain the Pareto front with the goal of high capture ratio and low energy spread. At last, one of the points in the Pareto front is selected to analyze single-particle motion.

DESIGN CONSIDERATIONS OF X-BAND LINAC

As mentioned in the last section, MOGA is a good choice for optimizing the TW tubes. For sake of applying the algorithm better, it is necessary to convert physics problems into mathematics problems reasonably.

Basic Theory

Designing the TW tubes with the iris-loaded waveguide structure requires the relationships between the field strength E and the power P, as a consequence of beam loading effect must be considered in actual operation，the relationships should be expressed as follows.

$$E(z) = \sqrt{2\alpha Z_s P(z)} \tag{1}$$

$$\frac{dP(z)}{dz} = -2\alpha P(z) - IE(z) \tag{2}$$

where α is the attenuation factor, Z_s is the shunt impedance, z is the longitudinal position in the TW tubes, and I is the average beam current.

As for Eq. (1) and (2), P is given at the beginning of the design, α and Z_s are determined by designing the structure according to the target field strength. α could be directly obtained by the two-dimensional electromagnetic field software SUPERFISH, while Z_s could be calculated by the group velocity v_g, the quality factor Q, and the angular frequency ω, stated as the following.

$$\alpha = \frac{\omega}{2v_g Q} \tag{3}$$

The above-mentioned field strength distribution should be designed according to the quality requirements of the

RECENT IMPROVEMENTS IN THE BEAM CAPTURE AT FERMILAB BOOSTER FOR HIGH INTENSITY OPERATION*

C. M. Bhat†, S. J. Chaurize, P. Derwent, M. W. Domeier, V. Grzelak, W. Pellico,
J. Reid, B. A. Schupbach, C.Y. Tan, A. K. Triplett, Fermilab, Batavia IL, USA

Abstract

The Fermilab Booster uses multi-turn beam injection with all its cavities phased such that beam sees a net zero RF voltage even when each station is at the same maximum voltage. During beam capture the RF voltage is increased slowly by using its paraphase system. At the end of the capture the feedback is turned on for beam acceleration. It is vital for present operations as well as during the PIP-II era that both the HLRF and LLRF systems provide the proper intended phase and RF voltage to preserve the longitudinal emittance from injection to extraction. In this paper, we describe the original architecture of the cavity phase distribution, our recent beam-based RF phase measurements, observed significant deviation in the relative phases between cavities and correction effort. Results from the improved capture for high intensity beam are also presented.

INTRODUCTION

Fermilab has undertaken major improvements to the existing accelerators in recent years to meet the high intensity proton demands for HEP experiments both onsite as well as long baseline neutrino experiments. An important program was the "Proton Improvement Plan" (PIP) [1, 2]. PIP had the baseline goal of extracting beam at 15 Hz from the Booster with about 4.3E12 ppp (protons per pulse). PIP completed its goals successfully in late 2016. During PIP-II [3], the plan is to increase the Booster beam intensity per cycle by >50%, and the cycle rate from 15 Hz to 20 Hz. The injection energy will be increased from 400 MeV to 800 MeV by using a newly built superconducting RF LINAC which will be completed around 2027. We have an intermediate beam intensity goal of achieving ~5E12 ppp in about two years. This will enable us to increase the beam power on the NuMI target from 700 kW to >900 kW. Concurrently, we will continue to provide 8 GeV beam to multiple low energy neutrino experiments before PIP-II comes online. The intermediate power increase helps us to better prepare Booster for the PIP-II era.

Booster is the oldest rapid cycling synchrotron (RCS) in operation in the world. Mitigation of beam losses during current operations continue to be a challenge and is of high priority. The allowed beam loss must be ≲475 W in the Booster ring or an average 1 W/m during its operation. Figure 1 displays a typical snapshot of the RF voltage, beam current and beam loss from its current operation.
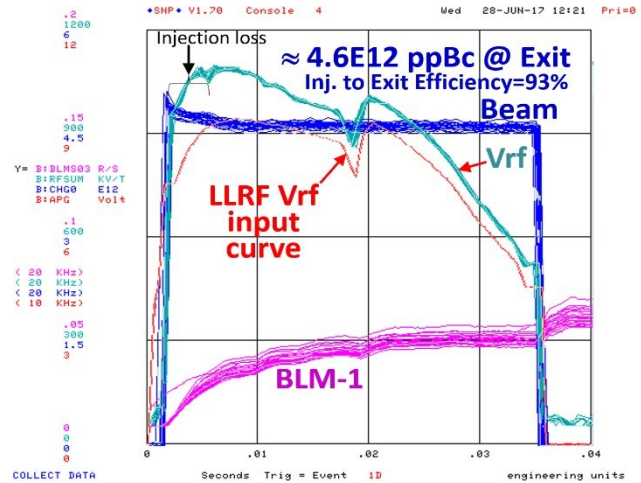

Figure 1: These are snapshots of the RF voltage, beam current, and a beam loss monitor at every 15 Hz tick.
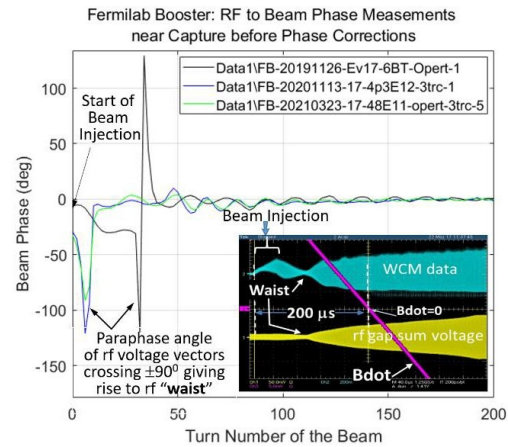

Figure 2: RF to beam phase measurements during injection and capture. The inset shows the wall current monitor (WCM) data (cyan), RF waveform (yellow), Bdot curve (magenta) during the first 400 μs of the beam cycle.

The Booster beam cycle starts with a multi-turn H⁻ injection scheme with no RF buckets opened. The injected beam debunches and loses its LINAC bunch structure by the end of beam injection. Next, the injected beam is captured by raising the RF voltage by changing the phase angle between two groups of RF cavities called A and B (see Figs. 3(a), 3(b)). A and B have the same number of RF stations (see Fig. 4). This method of manipulating the phase is called RF *paraphase*.

Since 2015 we have adopted an early injection scheme [4] by adding ~200 μs to the beam cycle for adiabatic beam capture. The aim is to improve the capture efficiency and reduce any beam loss arising from longitudinal beam dynamics dur-

LONGITUDINAL EMITTANCE MEASUREMENT AT PIP2IT*

Mathias El Baz†, Université Paris Saclay, Orsay, France
Jean-Paul Carneiro, Fermilab, Batavia, USA

Abstract

The PIP-II particle accelerator is a new upgrade to the Fermilab accelerator complex, featuring an 800 MeV H⁻ superconducting linear accelerator that will inject the beam into the present Fermilab Booster. A test accelerator known as PIP-II Injector Test (PIP2IT) has been built to validate the concept of the front-end of PIP-II [1]. One of the paramount challenges of PIP2IT was to demonstrate a low longitudinal emittance at the end of the front end. Having a low longitudinal emittance is crucial in order to ensure the stability of the beam in the accelerator. We present a longitudinal emittance measurement performed at 14.3 MeV by scanning the SSR1-8 cavity phase and measuring the corresponding beam rms bunch length with a Fast Faraday Cup (FFC) located in the High Energy Transport line (HEBT). The FFC signal is recorded by a high-bandwidth oscilloscope.

INTRODUCTION

The PIP-II Injector Test facility (PIP2IT) is a model of the Front End of PIP-II which will accelerate the H⁻ ion beam up to 25 MeV. As shown in Fig. 1, the injector is made of an Ion Source, a Low Energy Beam Transport (LEBT) made of three solenoids that matches the beam into a 162.5 MHz Radiofrequency Quadrupole (RFQ), a Medium Energy Beam Transport (MEBT) that prepares the beam for injection into two superconducting (SC) cryomodules: one containing eight Half-Wave Resonators (HWR) cavities operating at 162.5 MHz and one containing eight Single-Spoke Resonator (SSR1) cavities operating at 325 MHz. At the end of the injector a High-Energy Beam Transport (HEBT) brings the beam to a dump.
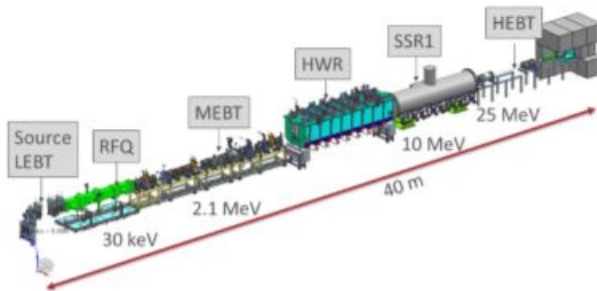

Figure 1: Sketch of PIP2IT.

During normal operation of the injector, the ion source operates with long pulses (usually few ms) and at 20 Hz repetition rate. A beam chopper, located upstream of the third LEBT solenoid, cut pulses of up to 0.55 ms of beam at

a repetition rate of 20 Hz. At the exit of the RFQ, the beam has an energy of 2.1 MeV. The MEBT has two purposes: first the MEBT performs a bunch-by-bunch selection using two kickers that decreases the average current in the macro-pulse from 5 mA down to 2 mA, and second the MEBT matches the beam into the HWR cryomodule using 3 buncher cavity (operating at 162.5 MHz), 2 doublets and 7 triplets. During normal operation, the beam is expected to reach an energy of 10.3 MeV at the exit of the HWR cryomodule and 25 MeV at the exit of the SSR1 cryomodule. The transverse focusing is performed by 8 SC solenoids in the HWR cryomodule and by 4 SC solenoid in the SSR1 cryomodule. The HEBT is made of 2 quads.

The goal of the longitudinal emittance measurement performed at PIP2IT is to quantify the beam quality at the end of the injector. A low longitudinal emittance ensures a small bunch length and little variations of the longitudinal momentum inside the bunch, and therefore, a high stability of the beam with negligible losses along the PIP2 linac.

MEASUREMENT SCHEME

Injector Settings

During the commissioning of the PIP2IT injector (from Spring 2020 to Spring 2021), the 3 first HWR cavities were not operational because of a frequency offset for the two first cavities and a coupler issue for the third one. Furthermore, due to multipacting effects, the 2 last HWR cavities (HWR#7 and #8) were operated at lower accelerating gradient than originally anticipated (respectively 8.5 MV/m and 8 MV/m vs 9.7 MV/m). As a consequence of these HWR cavities adjustments, the beam was longitudinally matched from the MEBT into the fourth HWR cavity reaching a beam energy of 8 MeV at the end of the HWR cryomodule and further accelerated to 16.2 MeV by the SSR1 cryomodule. During our longitudinal emittance measurement, and in order to lower the beam power in the Fast Faraday Cup (FFC), the pulse length was limited to 10 µs and the repetition rate to 1 Hz. The average beam current of 5 mA at the exit of the RFQ was chopped down to 2 mA by the 2 MEBT kickers. Under these conditions, the beam was transported with minimal uncontrolled losses until the dump at the end of the HEBT.

Beam Dynamic Simulations

Figure 2 shows the transverse and longitudinal envelope along the PIP2IT injector from Tracewin [2] for the above-mentioned injector settings used during the longitudinal emittance measurement. The simulation starts with a 792×10^3 input distribution at the MEBT ($z = 0$ in Fig. 2). This input distribution was built from a start-to-end model of the Ion Source, LEBT and RFQ, this later being simulated using

STATUS OF THE JAEA-ADS SUPERCONDUCTING LINAC DESIGN

B. Yee-Rendon*, Y. Kondo, J. Tamura, S. Meigo and F. Maekawa
JAEA/J-PARC, Tokai-mura, Japan

Abstract

The Japan Atomic Energy Agency (JAEA) is working in the research and development of an Accelerator Driven Subcritical System (ADS) for the transmutation of nuclear waste. To this end, JAEA is designing a 30 MW cw proton linear accelerator (linac) with a beam current of 20 mA. The JAEA-ADS linac starts with a Normal Conducting (NC) up to an energy of 2.5 MeV. Then, five Superconducting (SC) sections accelerate the beam up to 1.5 GeV. The biggest challenge for this ADS linac is the stringent reliability required to avoid thermal stress in the subcritical reactor, which is higher than the achieved in present accelerators. For this purpose, the linac pursues a strong-stable design that ensures the operation with low beam loss and fault-tolerance capabilities to continue operating in case of failure. This work presents the beam dynamics results toward achieving high reliability for the JAEA-ADS linac.

INTRODUCTION

The Japan Atomic Energy Agency (JAEA) is doing R&D in an Accelerator Driven Subcritical System (ADS) for the transmutation of minor actinides to reduce the long lifetime and high radiotoxicity of nuclear waste. The JAEA-ADS project is composed of a 30 MW cw proton linac, a spallation target, and an 800 MW thermal power subcritical reactor [1], as shown in Fig. 1.
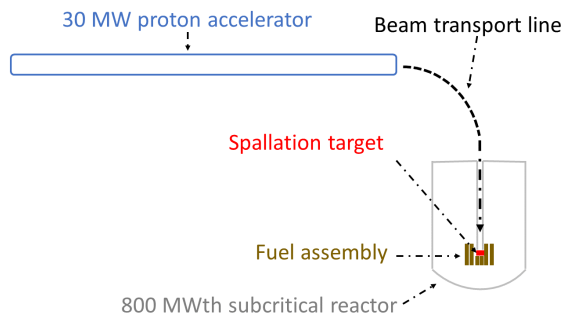

Figure 1: General scheme for the ADS.

A summary of the main specifications of the JAEA-ADS linac is provided in Table 1. Among them, the restricted number of beam trips is the main challenge for the ADS, which is beyond the present high-intensity linacs [2]. Thus, the JAEA-ADS linac seeks a reliability-oriented accelerator by achieving a robust beam optics design and fault-tolerance capabilities [3].

BEAM OPTICS DESIGN

The beam optics design pursues strict control beam loss and beam properties such as energy spread and emittance

Table 1: Main Characteristics of the JAEA-ADS Accelerator

Parameter		Beam trip duration
Particle	Proton	
Beam current (mA)	20	
Beam energy (GeV)	1.5	
Duty factor (%)	100 (cw)	
Beam loss (W/m)	< 1	
Length (m)	429	
Beam trips per year [4]	2×10^4	$\leq$ 10 s
	2×10^3	from 10 s to 5 min
	42	> 5 min

growth; simple lattice arrangement; operation with de-rated elements to reduce the failure probabilities and applied fault-tolerance schemes.

Figure 2 shows that JAEA-ADS linac has a normal conducting (NC) part, a so-called Injector, and a superconducting (SC) part known as the Main Linac. The Main Linac employs five groups of SC cavities to achieve high accelerating efficiency and compact design. The Half Wave Resonator (HWR) and Single Spoke Resonator (SSR) use a configuration solenoid-cavity inside the cryomodule. For the HWR region, the period is composed of one solenoid and one cavity; on the contrary, the SSR periods have two SC cavities for SSR1 and three for SSR2. Five-cell Elliptical Resonators (EllipRs) employ doublet NC quadrupoles with three and five SC cavities per cryomodule for EllipR1 and EllipR2, respectively [5].
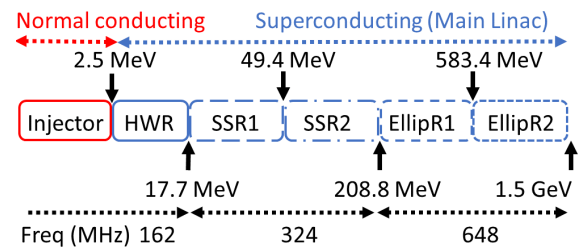

Figure 2: Linac lattice configuration.

At the normal operation, the maximum accelerating gradient (E_{acc}) for the SC cavities was chosen to operate with an electric peak up to 30 MV/m to reduce the possibility of a malfunction in the cavity. Moreover, in case of an SC cavity failure, it enables the increase of E_{acc} to apply for fault-tolerance compensations.

The beam optics was developed using the programs GenLinWin and Tracewin [6]. The beam loss was minimized by reducing the beam halo and emittance growth. This was achieved by pursuing an equipartitioning model, avoiding parameter resonances, among others [5]. The lattice design was optimized first in ideal conditions, i.e., without errors,

---

* byee@post.j-parc.jp

REDUCTION OF THE BEAM JITTER AT THE PIP2IT TEST ACCELERATOR*

A. Shemyakin†, G. Saewert, A. Saini, Fermilab, Batavia, IL 60510, USA

Abstract

Analysis of the beam position monitor (BPM) signals at the H- test linear accelerator PIP2IT showed that a large portion of the signals scatter comes from the beam jitter. BPM position measurements of the jitter modes were compared with beam orbit responses to perturbations excited by driving various beamline parameters in a low frequency sinusoidal manner. The main contributor to the jitter was found to be a low-frequency noise in the input reference to the ion source high voltage (HV) power supply. Filtering the HV power supply reference signal decreased the rms scatter in BPM readings by a factor of 2-3.

INTRODUCTION

The PIP-II Injector Test (PIP2IT) [1] was an H- ion linac that was assembled in several stages in 2014-2021 to test critical elements of the front end of the PIP-II accelerator currently under development at Fermilab [2]. In its final configuration (Fig. 1), the PIP2IT consisted of a 30 kV, 15 mA H- DC ion source, a 2 m long Low Energy Beam Transport (LEBT), a 2.1 MeV CW 162.5 MHz RFQ, a 10 m Medium Energy Beam Transport (MEBT), two cryomodules (HWR and SSR1) accelerating the beam up to 17 MeV, a High Energy Beam Transport (HEBT), and a beam dump.

Transverse focusing was provided by solenoids in the LEBT and cryomodules, and by quadrupole doublets and triplets in the MEBT and HEBT. Each doublet/triplet or solenoid (except in the LEBT) was accompanied by a BPM operating at 162.5 MHz.

The PIP2IT beam was operated in the pulse regime with 20 Hz repetition rate and the bunch population corresponding to the pulse current of 5 mA. The pulse duration varied up to 25 ms, but all measurements described in this paper were performed at 10 µs.

Soon after beginning of MEBT operation, it was observed that the pulse-to-pulse variation in the positions measured by BPMs significantly exceeded the expected electronics noise. The scatter was analysed, similar to what

has been reported before (e.g. see Ref. [3]), by simultaneous recording of signals from all BPMs for tens of minutes and applying Singular Value Decomposition (SVD) to the resulting matrix. The scatter was dominated by a single mode. The ratio between the first and second eigenvalues was found to be about 10, and the components beyond the second eigenvalue were already at the noise floor [4].

The first spatial eigenvector was found to be a linear combination of the MEBT betatron modes starting from the RFQ exit. It clearly indicated that the BPM position scatter was dominated by the beam jitter originated upstream of the MEBT. Initial attempts to identify the source of the jitter by checking parameters readbacks in the ion source and LEBT were unsuccessful because of a high level of noise in the reading channels themselves.

While additional analysis [5] showed that the increase in projected emittances due to the jitter is small, the BPM readings scatter did negatively affect quality of measurements. Consequently, in the final run of PIP2IT additional efforts were made to find and correct the source of the jitter.

CHARACTERIZATION OF BEAM JITTER

An example of beam jitter characterization is shown in Fig. 2. In this measurement, the beam was propagating to the middle of the MEBT at the energy of 2.1 MeV, and beam positions, averaged over a pulse, were recorded by horizontal (X) and vertical (Y) channels of 7 BPMs for 500 seconds at 20 Hz pulse rate. The typical rms scatter was about 0.1 mm (Fig. 2a). The resulting (m=10000) x (n=14) matrix M was decomposed with SVD in MathCad into a product of three matrixes:

$$M = ULV^T, \quad (1)$$

where L is a diagonal $n \times n$ matrix populated with eigenvalues ordered in the descending order; U is an $m \times n$ matrix composed of temporal eigenvectors, and V is a $n \times n$ matrix of spatial eigenvectors.

As Fig. 2b shows, the 1st eigenvalue exceeded the 2nd by a factor of 6. The Fourier spectrum of the 1st temporal
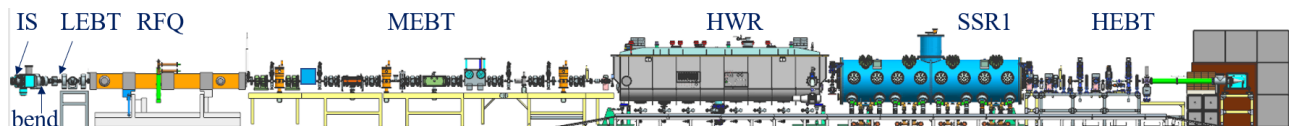

Figure 1: Side view of the PIP2IT.

eigenvector (Fig. 2c) is composed mainly by low-frequency (< 4 Hz) components, with a prominent peak at 1.1 Hz. While this peak was not a dominant contributor to the rms jitter value, it was a convenient marker to match while looking for the noise source. To describe the spatial

RESONANCE COMPENSATION FOR HIGH INTENSITY AND HIGH BRIGHTNESS BEAMS IN THE CERN PSB

F. Asvesta*, S. Albright, F. Antoniou, H. Bartosik, C. Bracco, G. P. Di Giovanni,
E. H. Maclean, B. Mikulec, T. Prebibaj[1], E. Renner[2]
CERN, Geneva, Switzerland
[1]also at Goethe University, Frankfurt, Germany, [2]also at TU Wien, Vienna, Austria

Abstract

Resonance studies have been conducted during the recommissioning of the CERN Proton Synchrotron Booster (PSB) following the implementation of the LHC Injectors Upgrade (LIU) project. In particular, resonance identification through so-called loss maps has been applied on all four rings of the PSB, revealing various resonances up to fourth order. In a second step, compensation schemes for the observed resonances were developed using a combination of analytical methods, experimental data and machine learning tools. These resonance compensation schemes have been deployed in operation to minimize losses for reaching high intensity and high brightness, thereby achieving the target brightness for the LHC-type beams.

INTRODUCTION

After the completion of the LIU project [1], the PSB faces the challenge of achieving the target values of twice the brightness for the LHC-type beams and increased intensity for the fixed target beams of the various physics users, such as ISOLDE [2] and n-TOF [3], as well as possible future users in the scope of the Physics Beyond Coliders (PBC) project [4]. The main limitations for reaching these goals come from space charge effects, which have been mitigated with the increase in injection energy achieved with the new linear accelerator, Linac4 [5], and the H^- charge exchange injection scheme [6, 7]. However, the β-beating introduced by the injection chicane in the first few ms [8] of the cycle, as well as betatron resonances excited by machine imperfections, still require careful correction for reaching the target beam parameters.

Extended resonance studies were conducted in the pre-LIU era to characterize the resonances, in all PSB rings, at the new injection energy of 160 MeV [9, 10]. The studies, which were used as a preparatory stage for a smoother recommissioning period, revealed several 3rd order normal and skew resonances. It should be noted that the four superposed rings did not behave the same in terms of resonances. For example, in Ring 4 only the normal sextupole resonance, $Q_x + 2Q_y = 13$, was observed while in Ring 3 all skew and normal 3rd order resonances resulted in losses. In addition, the compensation values for the same resonance in different rings, such as the half integer resonance excited in all rings, were different. However, the energy upgrade was only part of the LIU project. The newly installed elements, like the ones
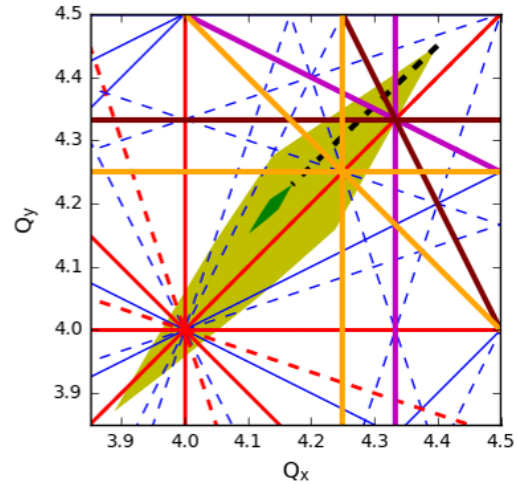
* foteini.asvesta@cern.ch

Figure 1: Schematic of the expected incoherent tune spreads at the PSB injection (yellow area) and extraction (green area) for the LHC-type beams. The tunes are varied during the cycle following the dotted black line. Resonance lines up to 4th order are plotted, normal in solid and skew in dashed. The non-systematic resonance lines are plotted in blue and the systematic in red. Potentially excited resonances of interest are highlighted in different colors depending on their order, 3rd order normal in purple, skew in brown and 4th order normal in orange.

needed for the new injection scheme, can have an impact on the excitation of the resonances and hence past studies can only offer an indication of the post-upgrade behaviour. Furthermore, the expected incoherent space charge tune spread at the PSB injection can be, in absolute value, larger than $|\Delta Q_{x,y}| > 0.5$ for the higher brightness beams [11,12]. Consequently, the tunes are set to high values at injection, for example $Q_x = 4.4$ / $Q_y = 4.45$ for these beams. The tunes are then varied during acceleration to reach the optimized extraction tunes of $Q_x = 4.17$ / $Q_y = 4.23$. Hence, the tune space of interest is large and multiple resonances are crossed during normal operation as shown in Fig. 1. In this respect, complete studies in order to identify and compensate any observed resonances were crucial during the commissioning phase to prepare the operational beams.

RESONANCE IDENTIFICATION

The resonance studies were one of the priorities of the commissioning period in the PSB, as multiple 2nd and 3rd

CHROMATICITY MEASUREMENT USING BEAM TRANSFER FUNCTION IN HIGH ENERGY SYNCHROTRONS

X. Buffat*, S.V. Furuseth, G. Vicentini, CERN, Geneva, Switzerland

Abstract

Control of chromaticity is often critical to mitigate collective instabilities in high energy synchrotrons, yet classical measurement methods are of limited use during high intensity operation. We explore the possibility to extract this information from beam transfer function measurements, with the development of a theoretical background that includes the impact of wakefields and by analysis of multi-particle tracking simulations. The investigations show promising results that could improve the operation of the HL-LHC by increasing stability margins.

INTRODUCTION

Operation with the lowest positive chromaticity is usually advised in high energy hadron synchrotrons (i.e. above transition) to both ensure the self-stabilisation of the rigid bunch mode while maximising the beam lifetime. In machines with a fast cycle, the chromaticity is often set empirically to the lowest value that does not result in instabilities. For machines with a long cycle, such as the Large Hadron Collider, this approach is time consuming. In addition, dynamic effects in superconducting magnets and lengthy beam optics operations may lead to strong variations of the chromaticity requiring dynamic corrections. In the LHC, the chromaticity is corrected through the cycle based on a measurement during a dedicated cycle featuring an energy modulation driven by the RF cavities. Such an energy modulation cannot be used with high intensity beams (i.e. multiple bunches) due to the large amount of beam losses generated. The operation with high intensity beams therefore relies on the corrections done with low intensity beams and the cycle-to-cycle reproducibility of the machine. The design chromaticity for the LHC is 2 units [1]. Figure 1 shows the octupole strength required to stabilise the beams, taking into consideration the residual noise that the beam experiences (dashed lines). We observe that the design chromaticity of 2 units is quite optimal to minimise the strength of the octupole required to stabilise the beams, while avoiding the potential adverse effects on the single particle dynamics that could occur at high chromaticity, e.g. around 20 units. However, this working point is close to the most critical configuration in terms of required octupole strength, i.e. around a chromaticity of 0. The cycle-to-cycle reproducibility is not enough to guarantee a sufficient stability of the chromaticity at the optimal working point. The operational working point was therefore set at 15 units [2], allowing for potential cycle-to-cycle variations in the order of ± 5 units. Due to this uncertainty, the optimal range of chromaticities, here around 3 units, cannot be exploited. Enabling this opportunity could reduce the

---
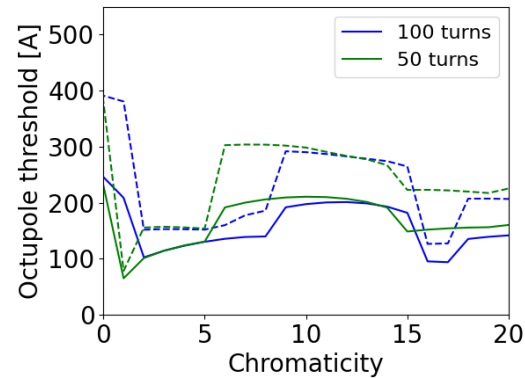
* xavier.buffat@cern.ch

Figure 1: Octupole current required for the stabilisation of the beam in the LHC in the configuration described in Table 1. The solid lines correspond to the octupole threshold obtained neglecting the impact of residual sources of noise on the beam (e.g. [3]), while the dashed lines take into account the destabilising effect of noise [4]. The blue and green curves are labelled with the corresponding damping time of the active feedback.

need for octupole strength by about a factor 2, thus offering significant operational margins, e.g. in terms of control of linear coupling or residual lattice nonlinearities, which need to be compensated with more strength in the arc octupoles to maintain Landau damping [5]. Alternatively, this might also allow for a reduction of the collimator gaps, thus improving the cleaning efficiency.

We observe in Fig. 1 that the width of this range of chromaticities featuring minimal octupole requirement depends on the gain of the transverse damper. In addition, the non-Gaussian modifications of the longitudinal distribution caused by the active blowup during the ramp [6] may significantly narrow down the range of optimal chromaticities [7]. To exploit this optimal working point, we therefore seek a chromaticity measurement technique that features a low level of beam losses, even during high intensity operation, and an accuracy in the order of 1 unit. The Beam Transfer Function (BTF) appears as a good candidate, since it contains information about the chromaticity [8] and it can be measured with a transverse excitation affecting a single bunch among a fully filled machine thanks to fast kickers and pickups. After a brief reminder of important theoretical aspects of the BTF and a description of our numerical model, we shall describe different ways to extract the chromaticity from the BTF measurement, identifying their strengths and shortcomings based on their application to simulation data.

RECENT PROGRESS ON NONLINEAR BEAM MANIPULATIONS IN CIRCULAR ACCELERATORS

A. Bazzani, F. Capoani[1], Bologna University and INFN, Bologna, Italy
M. Giovannozzi[*], CERN Beams Department, Geneva, Switzerland
[1]also at CERN Beams Department, Geneva, Switzerland

Abstract

In recent years, transverse beam splitting by crossing a stable resonance has become the operational means to perform MultiTurn Extraction (MTE) from the CERN PS to the SPS. This method delivers the high-intensity proton beams for fixed-target physics at the SPS. More recently, further novel manipulations have been studied, with the goal of devising new techniques to manipulate transverse beam properties. AC magnetic elements can allow beam splitting to be performed in one of the transverse degrees of freedom. Crossing 2D nonlinear resonances can be used to control the sharing of the transverse emittances. Furthermore, cooling the transverse emittance of an annular beam can be achieved through an AC dipole. These techniques will be presented and discussed in detail, considering future lines of research.

INTRODUCTION

Nonlinear effects introduce new phenomena in beam physics. In recent years, they have been used extensively to design novel beam manipulations in which the transverse beam distribution is modified in a controlled way for different purposes. This is the case for the beam splitting that is at the heart of the CERN Multiturn Extraction (MTE) [1–4].

The possibility of a controlled manipulation of the phase space by means of an adiabatic change of a parameter opened the road-map to new applications in accelerator and plasma physics [1, 5–9]. In particular, the adiabatic transport performed by means of nonlinear resonance trapping allows manipulation of a charged particle distribution, as to minimize the particle losses during the beam extraction process in a circular accelerator. Furthermore, the control of the beam emittance can be obtained by a similar approach [4, 10, 11]. The experimental procedures [4, 10, 11] require a very precise control of the efficiency of the adiabatic trapping into resonances [12–14], as well as of the phase-space change during the adiabatic transport, when a parametric modulation is introduced by means of an external perturbation. All these processes can be represented by multi-dimensional Hamiltonian systems or symplectic maps [15].

The adiabatic theory for Hamiltonian systems is a key breakthrough towards an understanding of the effects of slow parametric modulation on the dynamics. The concept of adiabatic invariant allows the long-term evolution of the system to be predicted and the fundamental properties of the action variables to be highlighted upon averaging over the fast variables [16, 17]. The theory has been well developed

for systems with one degree of freedom [12, 18–21], but the extension of some analytical results to multi-dimensional systems or to symplectic maps [22] has to cope with the issues generated by the ubiquitous presence of resonances in phase space [23, 24]. For these reasons, such an extension is still an open problem.

The combination of nonlinear effects that do not preserve the linear Courant-Snyder invariant, and adiabatic variation of the system parameters that allow crossing separatrices, opens new regimes that can be used to propose novel beam manipulations, in which essential beam parameters, such as the emittances can be changed in a controlled way.

In this paper, three novel beam manipulations are reviewed, namely beam splitting by means of AC elements [25], sharing of transverse emittances by crossing a nonlinear 2D resonance [26], and cooling of an annular beam distribution [27, 28].

ADIABATIC THEORY OF SEPARATRIX CROSSING

Phenomena occurring when a Hamiltonian system is slowly modulated have been widely studied in the framework of adiabatic theory [18, 19]. As the modulation of the Hamiltonian changes the shape of the separatrices in phase space, the trajectories can cross separatrices and enter into different stable regions associated with nonlinear resonances. The separatrix crossing can be described in a probabilistic way due to the sensitive dependence on initial conditions, and the crossing probabilities can be computed in the adiabatic limit, like the change of adiabatic invariant due to the crossing [18, 19].

Let us consider a Hamiltonian $\mathcal{H}(p, q, \lambda = \epsilon t)$, $\epsilon \ll 1$, where the parameter λ is slowly modulated and whose phase space is sketched in Fig. 1. An initial condition in Region III has a probability to be trapped into Region I or II of phase space given by [18]
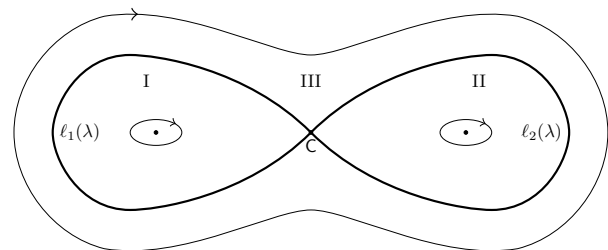

Figure 1: A generic phase-space portrait divided into three regions (I, II, III) by separatrices $\ell_1(\lambda)$ and $\ell_2(\lambda)$.

* massimo.giovannozzi@cern.ch

HL-LHC BEAM DYNAMICS WITH HOLLOW ELECTRON LENSES

P. D. Hermes*, R. Bruce, R. De Maria, M. Giovannozzi, A. Mereghetti†, D. Mirarchi, S. Redaelli
CERN Beams Department, Geneva, Switzerland
G. Stancari
Fermi National Accelerator Laboratory, Batavia, Illinois, USA

Abstract

Each of the two proton beams in the High-Luminosity Large Hadron Collider (HL-LHC) will carry a total energy of 700 MJ. One concern for machine protection is the energy stored in the transverse beam halo, estimated to potentially reach up to 5% of the total stored energy. Several failure scenarios could drive this halo into the collimators, potentially causing damage and therefore severely affecting operational efficiency. Hollow Electron Lenses (HEL) were integrated in the HL-LHC baseline to mitigate this risk by depleting the tails in a controlled way. A hollow-shaped electron beam runs co-axially with the hadron beam over about 3 m, such that halo particles at large amplitudes become unstable, while core particles ideally remain undisturbed. Residual fields from electron beam asymmetries can, however, induce emittance growth of the beam core. Various options for the pulsing of the HEL are considered and are compared using two figures of merit: halo depletion efficiency and core emittance growth. This contribution presents simulations for these two effects with different HEL pulsing modes using updated HL-LHC optics, that was optimized at the location of the lenses.

INTRODUCTION

Small fractions of the large stored beam energy in HL-LHC [1] can potentially cause severe damage to the machine hardware and negatively impact the operational efficiency, if they are lost in an uncontrolled way. The Large Hadron Collider (LHC) [2] is already equipped with a sophisticated, multi-stage collimation system [3–5] to intercept particles at large betatron or momentum offsets before they are lost in the sensitive LHC hardware. The highly-populated beam halo poses additional concerns that the upgraded HL-LHC collimation system [6] might not be able to cope with.

Assuming that up to 5% of the stored beam energy can be located in the halo of the circulating proton beams [7, 8], some of the failure scenarios that may occur in HL-LHC [9, 10] put at risk the integrity of the collimation system itself, with potentially severe consequences for the scientific programme. Most notably, for the context of this work, machine safety is endangered by sudden orbit shifts which would steer the highly populated beam halo into the primary collimators, that are closest to the circulating beams. Overall, the collimation system must work safely, also with sudden orbit shifts in the order of $2\,\sigma$ (with σ being the RMS beam size).

---

* pascal.hermes@cern.ch
† Currently at Fondazione CNAO, Strada Campeggi 53, 27100 Pavia, Italy

Hollow electron lenses (HEL) have recently been added to the upgrade baseline of the HL-LHC [6] to mitigate effects of highly-populated beam halo through an active control of its halo population. This paper reviews the key parameters of the HELs and gives a status update of the beam dynamics simulations for the halo depletion efficiency and the impact of residual fields on the emittance of the beam core.

HOLLOW ELECTRON LENSES FOR HL-LHC COLLIMATON

Hollow Electron Beam Parameters

The HEL [11] is a device that can actively remove particles at large transverse amplitudes, and thus deplete the halo in a controlled way. For this purpose, a hollow-shaped electron beam (see Fig. 1) is created and guided through a magnetic system in which the hadron and electron beams run co-axially over a certain length. The electron beam distribution is characterized by an inner and outer radius r_1 and r_2, respectively. Hadron particles moving through the HEL with a transverse amplitude smaller than r_1 are ideally unaffected, because the net electric and magnetic fields generated by the surrounding electron current yield zero. Hadrons with larger amplitudes than r_1 are subject to electric and magnetic fields which change their transverse momentum. This kick $\theta(r)$ is a function of the radius $r = \sqrt{x^2 + y^2}$ of the particle and can be quantified as follows

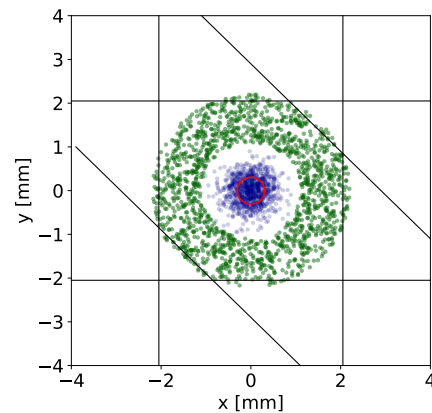$$\theta(r) = f(r)\,\theta_{\max}\left(\frac{r_2}{r}\right), \qquad (1)$$

Figure 1: Transverse distribution of the hollow electron beam (green) and the hadron beam (blue) at the HEL. The black lines indicate the cut generated by the primary collimators. The red circle corresponds to one RMS beam size.

MOP09

CLOSED FORM FORMULAS FOR THE INDIRECT SPACE CHARGE WAKE FUNCTION OF AXISYMMETRIC STRUCTURES

N. Mounet[*], C. Zannini, E. Dadiani[1], E. Métral, CERN, Geneva, Switzerland
A. Rahemtulla[2], EPFL, Lausanne, Switzerland
[1]now at Carnegie Mellon University, Pennsylvania, USA, and Tbilisi State University, Georgia
[2]now at ETHZ, Zurich, Switzerland

Abstract

Indirect space charge contributes significantly to the impedance of non-ultrarelativistic machines such as the LEIR, PSB and PS at CERN. While general expressions exist in frequency domain for the beam coupling impedance, the time domain wake function is typically obtained numerically, thanks to an inverse Fourier transform. An analytical expression for the indirect space charge wake function, including the time dependence as a function of particle velocity, is nevertheless highly desirable to improve the accuracy of time domain beam dynamics simulations of coherent instabilities. In this work, a general formula for the indirect space charge wake function is derived from the residue theorem. Moreover, simple approximated expressions reproducing the time and velocity dependence are also provided, which can even be corrected to recover an exact formula, thanks to a numerical factor computed once for all. The expressions obtained are successfully benchmarked with a purely numerical approach based on the Fourier transform.

INTRODUCTION

In high intensity synchrotrons, electromagnetic fields created by the beam passage through its interaction with its surroundings, is one of the main collective effect that can limit the performance of the machine, potentially leading to detrimental consequences such as heat load, emittance growth or, in the most dramatic cases, beam instabilities. Its role was pointed out as early as in 1965 in the seminal work of Laslett et al [1], and the concept of beam coupling impedance introduced slightly later by Sessler and Vaccaro [2]. The impedance, defined as the Fourier transform of the integrated force, felt by a witness (trailing) charge as a consequence of the interaction of a source (leading) charge with a certain accelerator equipment, normalised to the excitation, proved to be a very useful descriptor of the magnitude of such effects in a given machine. In particular, it can be efficiently used in Vlasov equation solvers to compute and predict instabilities.

Over the past fifty years many analytical formulas have been derived to provide such impedances, in particular in the case of a smooth, axisymmetric structure such as a vacuum pipe, made of one or several layers of materials in the radial direction [3–15]. On the other hand, the equivalent time domain quantity, namely the wake function [16][1], remains elusive, at least in the form of analytic formulas: for

cylindrical resistive geometries one can mention the famous thick-wall formula [5], its extension to non-ultrarelativistic beams [17], as well as a thin-wall formula [18].

As a matter of fact, even the simplest case of a perfectly conductive, cylindrical beam pipe, often called the indirect space charge (ISC) impedance, although well-known in frequency domain [8] still lacks a formula for its wake function—one can mention the ultrarelativistic expression by Chao [5], which is of limited practical interest as it is expressed as a Dirac delta function in the longitudinal coordinate along the bunch z. A more general wake function formula would nevertheless be useful when performing macroparticle simulations. In particular, in low-energy machines, the ISC is strong and its broad-band nature makes it very peaked close to $z = 0$ (the position of the source particle creating the wake), which in turn requires a very fine discretization along z, leading to time-consuming simulations. A simple analytical formula would therefore be highly beneficial to macroparticle simulations.

The ISC impedance is traditionally separated from the direct space charge (i.e. the impedance in free space), the latter being fundamentally of non-linear nature. In an axisymmetric structure, the longitudinal and transverse dipolar ISC impedances can be expressed respectively as [8]:

$$Z_{\parallel}(\omega) = \frac{i\omega\mu_0 L}{2\pi\beta^2\gamma^2} \frac{K_0\left(\frac{kb}{\gamma}\right)}{I_0\left(\frac{kb}{\gamma}\right)}, Z_{\perp}^{dip}(\omega) = \frac{ik^2 Z_0 L}{4\pi\beta\gamma^4} \frac{K_1\left(\frac{kb}{\gamma}\right)}{I_1\left(\frac{kb}{\gamma}\right)}, \tag{1}$$

with i the imaginary unit, b the radius of the pipe, L its length, $\omega > 0$ the angular frequency (in rad/s), μ_0 the vacuum permeability, $Z_0 = \mu_0 c$ the free space impedance, c the speed of light in vacuum, $v = \beta c$ the beam velocity, γ the relativistic mass factor, $k \equiv \omega/v$ the wave number, and I_0, I_1, K_0 and K_1 modified Bessel functions of the first and second kinds. Note that SI units are used throughout these proceedings.

In the following sections we will provide expressions for the ISC wake functions, defined as Fourier integrals:

$$W_{\parallel}(z) = \frac{1}{2\pi} \int_{-\infty}^{\infty} d\omega e^{i\omega\frac{z}{v}} Z_{\parallel}(\omega), \tag{2}$$

$$W_{\perp}^{dip}(z) = -\frac{i}{2\pi} \int_{-\infty}^{+\infty} d\omega e^{i\omega\frac{z}{v}} Z_{\perp}^{dip}(\omega). \tag{3}$$

---

* nicolas.mounet@cern.ch
[1] The wake function should not to be confused with the so-called wake potential that represents the convolution of the wake function by the

longitudinal bunch distribution. In early works (and in particular in Ref. [16]), the wake function was actually often called "wake potential".

CONTROLLED LONGITUDINAL EMITTANCE BLOW-UP FOR HIGH INTENSITY BEAMS IN THE CERN SPS

D. Quartullo*, H. Damerau, I. Karpov, G. Papotti,
E. Shaposhnikova, C. Zisou, CERN, Meyrin, Switzerland

Abstract

Controlled longitudinal emittance blow-up will be required to longitudinally stabilise the beams for the High-Luminosity LHC in the SPS. Bandwidth-limited noise is injected at synchrotron frequency sidebands of the RF voltage of the main accelerating system through the beam phase loop. The setup of the blow-up parameters is complicated by bunch-by-bunch differences in their phase, shape, and intensity, as well as by the interplay with the fourth harmonic Landau RF system and transient beam loading in the main RF system. During previous runs, an optimisation of the blow-up had to be repeated manually at every intensity step up, requiring hours of precious machine time. With the higher beam intensity, the difficulties will be exacerbated, with bunch-by-bunch differences becoming even more important. We look at the extent of the impact of intensity effects on the controlled longitudinal blow-up by means of macro-particle tracking, as well as analytical calculations, and we derive criteria for quantifying its effectiveness. These studies are relevant to identify the parameters and observables which become key to the operational setup and exploitation of the blow-up.

INTRODUCTION

The "High Luminosity LHC" (HL-LHC) proton beams in the SPS will require stabilization in the longitudinal plane [1–3]. A fourth harmonic 800 MHz RF system in combination with the 200 MHz accelerating one will increase the synchrotron frequency spread inside the bunch enhancing Landau damping [4], whereas controlled blow-up will increase the bunch longitudinal emittance in a controlled way [5]. Both methods will be required to cope with coupled-bunch instabilities along the ramp and at flat-top.

Controlled emittance blow-up is achieved in the SPS by injecting bandwidth-limited phase noise into the phase-loop of the main RF system [6], as done also in the CERN PSB and LHC [7–10]. Phase noise should diffuse just the particles situated in the bunch core, since affecting the tails could lead to particle losses. Emittance blow-up should occur along the SPS ramp, so that particles driven out of the buckets are lost in the SPS, and are not transferred to the LHC.

The noise-generation algorithm produces digital, band-limited phase noise samples. Since the frequency band should cover the synchrotron frequencies of the particles situated in the bunch core, it must follow the changes of synchrotron frequencies during the ramp. The noise generation algorithm receives the required frequency band as input and produces phase noise with the desired spectral properties.

---

* danilo.quartullo@cern.ch

One main remaining issue is the determination of the optimal frequency band. A dedicated algorithm has been developed for this purpose. The frequency band is obtained by designing the emittance increase during blow-up and by making use of accurately computed synchrotron-frequency distributions, which include collective effects.

Longitudinal beam dynamics simulations of the SPS cycle are important to validate the effectiveness of the computed frequency bands. One batch of 72 bunches was tracked including the full SPS impedance model, beam loops and emittance blow-up. Simulations were then compared with beam measurements during the SPS cycle. The computed frequency bands provided useful input to set the phase-noise parameters with beam.

In this paper we describe the implementation of emittance blow-up in operation. Then, the procedure for the determination of the phase-noise frequency band is explained in detail. Results from beam dynamics simulations are reported and compared with first beam measurements.

IMPLEMENTATION OF THE PHASE-NOISE ALGORITHM

The HL-LHC beam requirements drove the LHC Injector Upgrade Project [11], which, at the SPS, foresaw a complete renovation of the RF system, including a rearrangement of the 200 MHz accelerating structures, and a redesign of the Low Level controls (LLRF, [12]), based on the MicroTCA platform, and featuring a restructuring of the beam control loops. The controlled emittance blow-up was operational for LHC-type beams in previous runs (2010-2018) [6], and had to be re-implemented in the new LLRF system. The addition of the noise in the phase loop is now done in the new, digital LLRF, but the previous algorithm for the preparation of the noise pattern and the high level controls are maintained.

The noise algorithm [13] creates an excitation spectrum that follows the varying frequency spectrum during the energy ramp, and that is band-limited, with very low leakage. The noise frequency bands are calculated in the SPS high level controls (LHC Software Architecture, LSA), and sent to the C++ code that prepares the noise pattern. The central synchrotron frequency f_{s0} in double-RF system without intensity effects is automatically calculated in LSA. The low and high band-limits are obtained by multiplying the calculated f_{s0} by two knobs, so to scale them easily.

DETERMINATION OF THE PHASE-NOISE FREQUENCY BAND

A first algorithm for the determination of the frequency band has been developed. It does not require particle track-

UNDERSTANDING OF THE CERN-SPS HORIZONTAL INSTABILITY WITH MULTIPLE BUNCHES

C. Zannini*, H. Bartosik, M. Carlà[1], L. Carver[2], K. Li, E. Métral, G. Rumolo, B. Salvant, M. Schenk

CERN, 1211 Geneva, Switzerland

[1]now at ALBA, Barcelona, Spain

[2]now at ESRF, Grenoble, France

Abstract

At the end of 2018, an instability with multiple bunches has been consistently observed during high intensity studies at the CERN-SPS. This instability could be a significant limitation to achieve the bunch intensity expected after the LHC Injector Upgrade (LIU). Therefore, a deep understanding of the phenomena is essential to identify the best mitigation strategy. Extensive simulation studies have been performed to explore the consistency of the current SPS model, give a possible interpretation of the instability mechanism and outline some possible cures.

INTRODUCTION

Major modifications of the CERN-SPS took place during the Long Shutdown 2 (LS2) in the framework of the LHC injectors upgrade project (LIU) [1–3]. In particular, the RF system has been modified with the aim of providing the necessary RF power for compensation of beam loading, which was limiting the acceleration of LHC beams to an intensity of about 1.3×10^{11} protons per bunch (ppb) before the upgrade. The LIU upgrades of the RF system, together with the longitudinal impedance reduction, are expected to enable the acceleration of the future LHC beams to reach the target intensity of 2.3×10^{11} ppb at the CERN-SPS extraction. While such high intensity beams could not be accelerated before the upgrade, they could already be studied at injection energy. After a short description of measurement observations this paper summarises the simulation studies performed to build an understanding of the horizontal instability experienced at injection energy with high intensity LHC beams.

INSTABILITY MEASUREMENTS

During the 2015 scrubbing campaign with high intensity LHC beams (about 2.0×10^{11} ppb), a horizontal instability affecting the third and fourth batch of trains of 72 bunches was observed. Stabilization was possible with high chromaticity and octupoles.

Since 2017, an increased transverse damper gain at high frequency was available, but high chromaticity was still needed to stabilise the beam. If the chromaticity is not high enough, the unstable bunches exhibit head-tail motion as revealed by measurements with the SPS head-tail monitor. In particular, oscillation patterns of mode 1 were observed for horizontal normalised chromaticity ($\xi = Q'/Q$) settings

_____
* carlo.zannini@cern.ch

of $0.1 \leq \xi_H \leq 0.3$ and mode 2 for $0.3 \leq \xi_H \leq 0.5$. A mode 3 pattern has also been observed for $\xi_H \approx 0.5$.

At the end of 2018, dedicated measurements were performed to further characterise the instability and test some possible cures. Four batches of 48 bunches were used for these studies. No instability was observed for lower number of batches and bunch intensity up to 2.0×10^{11} ppb. The horizontal chromaticity was kept high (normalised chromaticity of $\xi_H \approx 0.5$) for the injection of the first three batches but lowered to $\xi_H \approx 0.05$ just before the injection of the fourth batch while the transverse damper was on during the entire cycle. The octupoles were adjusted in order to compensate the horizontal detuning with amplitude due to residual non-linearities of the machine (setting of kLOF = -0.2 m^{-4}).

With the operational batch spacing of 200 ns the intensity threshold of the instability was found to be 1.8×10^{11} ppb. Figure 1 (top) shows an example of the intensity evolution along the SPS injection plateau for two different chromaticity settings. Instability starts from the last batch and extends to the other batches for lower chromaticity. Bunches in the last batch exhibit significant losses in the top plot, while for lower chromaticity (bottom plot), the instability clearly extends to the second and third batch. The growth times associated to this instability are in the order of 100 turns, as observed from the head-tail monitor acquisitions or from the turn-by-turn data of the transverse damper pickups. However, their exact value strongly depends on the damper settings. The damper, which does not have enough bandwidth to suppress the mode 1-2 head-tail instability, can, however, significantly modify the growth rates of the instability. Depending on damper settings, a variation of the instability growth rates up to a factor of three has been observed. The instability growth rates versus chromaticity have been measured and will be compared with the mode expectations in the next section.

The effect of batch spacing on the instability was also studied by varying the gap between batches in steps of 50 ns. Fewer bunches are affected by the instability when increasing the batch spacing and no instability was observed for a batch spacing larger than 500 ns.

Finally, measurements of the stability limit as a function of chromaticity and octupole settings were performed. As before, four batches of 48 bunches were injected, where the chromaticity was kept high for the injection of the first three batches and then lowered just before the injection of the fourth batch. Figure 2 shows the obtained stability limits for an intensity of about 1.8×10^{11} ppb at injection. Positive

INFLUENCE OF TRANSVERSE MOTION ON LONGITUDINAL SPACE CHARGE IN THE CERN PS

A. Laut*, A. Lasheen, CERN, Geneva, Switzerland

Abstract

Particles in an intense bunch experience longitudinal self-fields due to space charge. This effect, conveniently described by geometric factors dependent on a particle's transverse position, beam size, and beam pipe aperture, is usually incorporated into longitudinal particle tracking on a per-turn basis. The influence of transverse betatron motion on longitudinal space charge forces is, however, usually neglected in pure longitudinal tracking codes. A dedicated tracking code was developed to characterize the CERN PS such that an effective geometric factor of a given particle could be derived from its transverse emittance, betatron phase advance, and momentum spread. The effective geometry factor is then estimated per particle by interpolation without the need for full transverse tracking and incorporated into the longitudinal tracker BLonD. The paper evaluates this effect under conditions representative of the PS, where space charge is dominant at low energy and progressively becomes negligible along the acceleration ramp. The synchrotron frequency distribution is modified and the filamentation rate is moreover increased, which could suggest a stabilizing space charge phenomenon.

INTRODUCTION

In the Proton Synchrotron (PS) at CERN, longitudinal space charge, defined in Eq. (1) as a beam coupling impedance, dominates other impedance sources at injection where protons are accelerated from a mildly relativist kinetic energy of $E_k = 2$ GeV to a highly relativistic $E_k = 26$ GeV. Proportional to the vacuum impedance Z_0, a geometry factor g, and inversely proportional with $\beta\gamma^2$ [1].

$$\frac{Z}{n} = -j\frac{Z_0}{\beta\gamma^2}g \qquad (1)$$

The space charge geometry factor g describes the longitudinal self fields based on the beam size and aperture [2]. For a particle within a long round beam of uniform transverse density, the geometry factor is often expressed by

$$g = \frac{1}{2} + \ln\frac{b}{a} - \frac{1}{2}\frac{r^2}{a^2}, \qquad (2)$$

where a describes the beam radius, b describes the radius of a conductive aperture, and r describes the particle's radial offset.

Throughout the PS, longitudinal space charge impedance and other purely reactive impedance sources with constant Z/n induce wakefield voltages V_W given by Eq. (3)

$$V_W = -\frac{i}{\omega_s}\frac{Z}{n}\frac{d\lambda}{d\tau}, \qquad (3)$$

* alexander.laut@cern.ch

where $n = f/f_s$, f_s being the revolution frequency of the synchronous particle, the time coordinate $\tau = t - t_s$ being relative to the synchronous particle, and $d\lambda/d\tau$ being the derivative of $\lambda(\tau)$ the longitudinal bunch profile. Because of the large range of longitudinal space charge observed in the PS throughout the acceleration ramp (Fig.1), the induced wakefield voltage will have a strong and varying influence on the longitudinal dynamics, potentially influencing longitudinal beam stability [3]. To reproduce these effects in simulation, it is important to accurately model space charge in the PS.
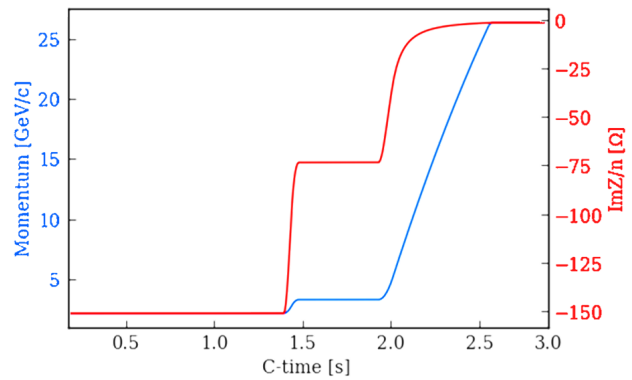

Figure 1: Space charge impedance $\text{Im}Z/n$ in the PS which dominates until it is compensated at higher momentum by the inductive impedance of the PS aperture of about 20 Ω [4].

The LHC Injectors Upgrade (LIU) project at CERN [5,6] aims to increase the total intensity of the injectors for both proton and ion beams to reach the requirements for High-Luminosity LHC (HL-LHC) [7]. At flat bottom where particle energies are lower, beam brightness is limited by space charge effects. In the transverse plane, charges within a bunch will repel each other, limiting the minimum transverse emittance. In the longitudinal plane, the self-fields of a bunch will be defocusing below transition energy, and focusing above. As a pure reactive impedance, longitudinal space charge will also influence Landau damping and overall beam stability.

As illustrated in Fig. 2, a bunch can spontaneously break up shortly after transition crossing due to high frequency impedance sources. Longitudinal space charge being a focusing force after transition, and being a function of $d\lambda/d\tau$, will amplify the modulation induced by wakefields.

MOP13

THE PS BOOSTER ALIGNMENT CAMPAIGN AND A NEW TUNE CONTROL IMPLEMENTATION AFTER THE LHC INJECTORS UPGRADE AT CERN

F. Antoniou*, F. Asvesta, H. Bartosik, J-F. Comblin, G. P. Di Giovanni, M. Hostettler, A. Huschauer, B. Mikulec, J. M. Nonglaton, T. Prebibaj[1], CERN, Geneva, Switzerland
[1]also at Goethe University, Frankfurt, Germany

Abstract

The CERN PS Booster (PSB) has gone through major upgrades during the Long Shutdown 2 (LS2) and the recommissioning with beam started in December 2020. Two of the aspects leading to improved operation will be described in this paper: a new tune control implementation; and a full re-alignment campaign. The operation of the PSB requires a large range of working points to be accessible, with a dynamic change of tunes along the acceleration cycle. Before LS2, the PSB tune control was based on an analytical approach assuming linear magnet transfer functions. As part of the LIU project, the PSB main power supply was upgraded to raise the extraction energy from 1.4 GeV to 2 GeV, in order to improve the brightness reach of the downstream machines. A new tune control implementation was necessary to take into account saturation effects of the bending magnets and the reconfiguration of the main circuits, as well as the additional complexity of the new H$^-$ charge exchange injection. The first part of the paper describes the implementation of the new tune control and its experimental verification and optimization. The second part describes the results of the PSB alignment campaign after LS2, giving emphasis to the method developed to perform a combined closed orbit correction through quadrupole alignments.

THE NEW PSB TUNE CONTROL

The operation of the PSB requires a large range of working points to be accessible, with a dynamic change of tunes along the acceleration cycle. Pre-LS2, the tune control implementation in the PSB was based on an analytical approach, which assumed linear magnet transfer functions [1]. This approach was proven to give a good agreement between the programmed and the measured machine tune with maximum discrepancies between the two of about $\Delta Q \approx 0.01$.

After LS2, the production of the high brightness LHC beams required a raise in the the PSB extraction energy from 1.4 GeV to 2 GeV in order to mitigate space charge effects in the PS. Therefore, the main power supply of the PSB was upgraded as part of the LIU project. Due to the higher operation energies, the main bending magnets of the PSB now operate in their saturation regime. To take into account the increased complexity due to the reconfiguration of the main circuits and the saturation effects of the bending magnets, as well as the additional impact of the new H$^-$ charge exchange injection [2], a new tune control scheme

* fanouria.antoniou@cern.ch

was implemented during LS2. This new implementation consists of three main modules:

1. The Q-editor application to set the tune functions along the cycle for each of the four rings of the PSB individually.

2. A make rule "Q → K" for determining the required quadrupole strengths (K) based on the requested tunes (Q). This is using the analytical description of the PSB lattice already employed pre-LS2.

3. A make rule for the translation from the required quadrupole strengths (K) to the respective power supply current (I), as well as the sharing of the power supply current among the different current circuits. This requires as input the calibration curves for the various magnets, taking into account the saturation at high currents and the differences between the magnet transfer functions for inner and outer rings.

The PSB Main Magnet Circuits

The configuration of the main magnet circuits of the PSB after LS2 is shown in Fig. 1 [3, 4]. It consists of:

- Two dipole circuits: one circuit common for all the bending magnets of the external rings (BR14) and all the 128 QFO focusing quadrupoles for all four rings. The current in this circuit will be denoted as $I_{b,\text{ext}}$. The other dipole circuit is common for all the bending magnets of the internal rings (BR23) and all the 64 QDE
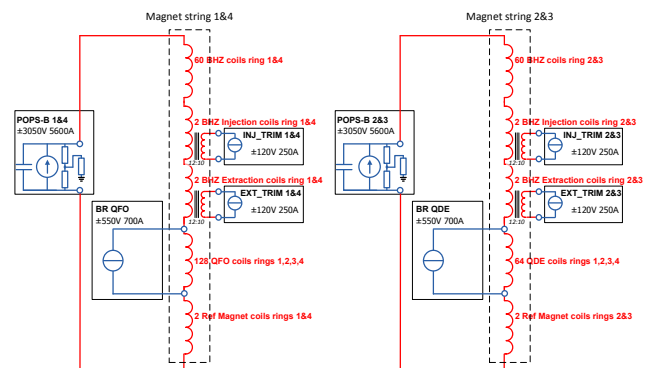

Figure 1: Main PSB power converter circuits after the LIU upgrade [3, 4].

THRESHOLD FOR LOSS OF LONGITUDINAL LANDAU DAMPING IN DOUBLE HARMONIC RF SYSTEMS

L. Intelisano*[1], H. Damerau, I. Karpov, CERN, Geneva, Switzerland
[1]Sapienza Università di Roma, Rome, Italy

Abstract

Landau damping is a natural stabilization mechanism to mitigate coherent beam instabilities in the longitudinal phase space plane. In a single RF system, binominal particle distributions with a constant inductive impedance above transition (or capacitive below) would lead to a vanishing threshold for the loss of Landau damping (LLD), which can be avoided by introducing an upper cutoff frequency to the impedance. This work aims at expanding the recent loss of Landau damping studies to the common case of double harmonic RF systems. Special attention has been paid to the configuration in the SPS with a higher harmonic RF system at four times the fundamental RF frequency, and with both RF systems in counter-phase (bunch shortening mode). Refined analytical estimates for the synchrotron frequency distribution allowed to extend the analytical expression for the loss of Landau damping threshold. The results are compared with semi-analytical calculations using the MELODY code, as well as with macroparticle simulations in BLonD.

INTRODUCTION

Landau damping [1] provides beam stability to a wide variety of working high beam intensity accelerators. In general, loss of Landau damping (LLD) occurs when the frequency of the coherent bunch oscillations moves outside the incoherent band. In the longitudinal plane, this natural stabilization mechanism is achieved by means of the synchrotron frequency spread which is caused by the nonlinearities of the RF fields. Synchrotron frequency spread, can be enhanced by using multiple RF systems. In particular, higher harmonic RF systems are operated in many accelerators either to change the bunch shape (even split it) or to increase the synchrotron frequency spread inside the bunch, as shown in Fig. 1. In this work we focused mainly on the Super Proton Synchrotron (SPS) configuration namely a 4th harmonic RF system (higher harmonic RF system at four times the fundamental RF frequency) and the case above transition energy. For such double harmonic RF systems, the total voltage seen by the particles is defined as:

$$V_{\text{RF}}(\phi) = V_0\big[\sin(\phi + \phi_{s_0}) + r\sin\left(n\phi + n\phi_{s_0} + \Phi_2\right)\big], \quad (1)$$

where V_0, r and ϕ_{s0} are respectively the voltage magnitudes of the main harmonic RF system, the voltage ratio between the higher harmonic and the fundamental harmonic RF system, and the phase of the synchronous particle. As far as ϕ, n and Φ_2 are concerned, they represent the phase offset with respect to the synchronous particle, the harmonic number
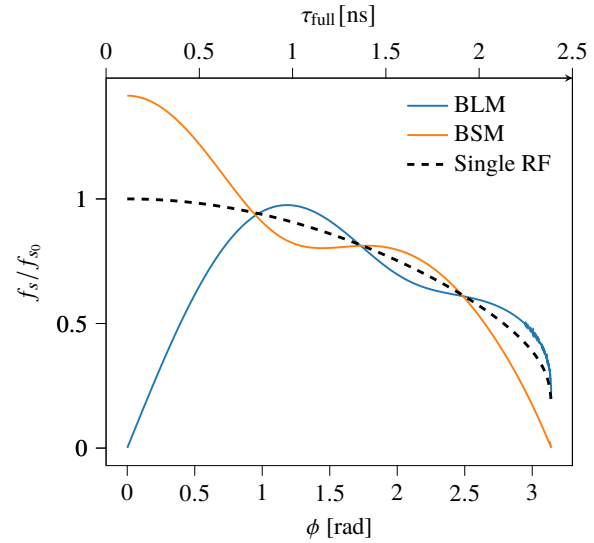
---
* leandro.intelisano@cern.ch

Figure 1: Synchrotron frequency spread normalized to the small-amplitude synchrotron frequency in a single RF system as a function of the maximum phase deviation of the particle. Two different operating modes for the 4th harmonic RF system are plotted, for the BSM (orange) and the BLM (blue) with $r = 0.25$. The curves are compared with the conventional single RF system case (black dashed line). The axis top concerning the full bunch length τ_{full} aims to be a reference for Fig 2.

ratio and the relative phase between the two RF systems. Depending on the relative Φ_2, two operating modes are defined; in particular in the case of two RF systems in phase, bunches would get shorter with respect to the single RF system case. This operating mode is called bunch shortening mode (BSM). On the other hand, in the case of both RF systems in counter-phase, one refers to the bunch lengthening operating mode (BLM).

Recent studies [2] prove that for a single RF system, binomial family of particle distributions with a constant inductive impedance $\text{Im}Z/k$ above transition energy, leads to a vanishing LLD threshold. However, this is avoidable by introducing an upper cutoff frequency f_c to the impedance. In the present work, an analytical expression of the LLD threshold in BSM, above transition energy, will be derived. Furthermore, its results will be compared with semianalytical calculations, using the MELODY code [3], and macroparticle simulations in BLonD [4]. Moreover, we will study the LLD by analyzing the offset evolution of the bunch after a rigid-dipole perturbation.

NEW ANALYTICAL CRITERIA FOR LOSS OF LANDAU DAMPING IN LONGITUDINAL PLANE

I. Karpov*, T. Argyropoulos, E. Shaposhnikova, CERN, Geneva, Switzerland
S. Nese, University of Bergen, Bergen, Norway

Abstract

Landau damping is a very important stabilization mechanism of beams in circular hadron accelerators. In the longitudinal plane, Landau damping is lost when the coherent mode is outside of the incoherent synchrotron frequency spread. In this paper, the threshold for loss of Landau damping (LLD) for constant inductive impedance $\mathrm{Im}Z/k$ is derived using the Lebedev matrix equation (1968). The results are confirmed by direct numerical solutions of the Lebedev equation and using the Oide-Yokoya method (1990). For more realistic impedance models of the ring, new definitions of an effective impedance and the corresponding cutoff frequency are introduced which allow using the same analytic expression for the LLD threshold. We also demonstrate that this threshold is significantly overestimated by the Sacherer formalism based on the previous definition of an effective impedance using the eigenfunctions of the coherent modes.

INTRODUCTION

The loss of Landau damping [1] has been observed in operations of different accelerators (Tevatron [2], RHIC [3], SPS [4] and LHC [5]) and has been studied for many years using different approaches [6–16]. A general way to analyze beam stability is to solve the Vlasov equation linearized for a small perturbation of a stationary particle distribution function. The first self-consistent system of equations suitable for the eigenvalue analysis of longitudinal beam stability was proposed by Lebedev in 1968 [6]. In the recent paper [17], we derived an analytic expression for the LLD threshold in the presence of the constant reactive impedance $\mathrm{Im}Z/k$ using the Lebedev equation. It agrees with the LLD threshold determined numerically by solving the two matrix equations: the Lebedev matrix equation and the Oide-Yokoya equation [18]. In this paper, we present the derivation of the LLD threshold which based on a novel method to compute an effective impedance with an effective cutoff frequency. This allows to evaluate the LLD threshold for complicated impedance models (like the one of the CERN SPS).

MAIN EQUATIONS AND DEFINITIONS

We consider the case of a single RF system, for the sake of simplicity, while the derivations can be adapted to other RF waveforms. The Lebedev equation can be written using variables $(\mathscr{E}, \psi)$, which correspond respectively to the energy and phase of the synchrotron oscillations,

$$\mathscr{E} = \frac{\dot{\phi}^2}{2\omega_{s0}^2} + U_t(\phi), \tag{1}$$

$$\psi = \mathrm{sgn}(\eta\Delta E)\frac{\omega_s(\mathscr{E})}{\sqrt{2}\omega_{s0}}\int_{\phi_{\max}}^{\phi}\frac{d\phi'}{\sqrt{\mathscr{E} - U_t(\phi')}}. \tag{2}$$

Here, ΔE and ϕ are respectively the energy and phase deviations of the particle from the synchronous particle, $\eta = 1/\gamma_{\mathrm{tr}}^2 - 1/\gamma^2$ is the slip factor, γ_{tr} is the Lorentz factor at transition energy, and $f_{s0} = \omega_{s0}/2\pi$ is the frequency of small-amplitude synchrotron oscillations in a bare RF potential. The total potential can be obtained from the sum voltage V_t

$$U_t(\phi) = \frac{1}{V_0\cos\phi_{s0}}\int_{\Delta\phi_s}^{\phi}\left[V_t(\phi') - V_0\sin\phi_{s0}\right]d\phi', \tag{3}$$

where V_0 is the RF voltage amplitude, and ϕ_{s0} is the synchronous phase. The synchronous phase shift due to intensity effects $\Delta\phi_s$ satisfies the relation $V_0\sin\phi_{s0} = V_0\sin(\phi_{s0} + \Delta\phi_s) + V_{\mathrm{ind}}(\Delta\phi_s)$, where V_{ind} is the induced voltage. In practice, U_t can be obtained for an arbitrary impedance model thanks to an iterative procedure [15]. Then it can be used to compute the synchrotron frequency as a function of the energy of synchrotron oscillations $\omega_s(\mathscr{E}) = 2\pi/T_s(\mathscr{E})$ in Eq. (2) from the period of oscillations including intensity effects.

Below we will consider particle distributions belonging to a binomial family $g(\mathscr{E}) = (1 - \mathscr{E}/\mathscr{E}_{\max})^\mu$. For a finite μ, which is usually the case for proton bunches, a full length τ_{full} is defined as

$$\tau_{\mathrm{full}} = \left[\phi_{\max}(\mathscr{E}_{\max}) - \phi_{\min}(\mathscr{E}_{\max})\right]/\omega_{\mathrm{RF}}. \tag{4}$$

Lebedev Equation

Using the variable and notations described above, an infinite system of equations for harmonics of the line density perturbation $\tilde{\lambda}$ at frequency Ω [6], can be written as

$$\tilde{\lambda}_p(\Omega) = -\frac{\zeta}{h}\sum_{k=-\infty}^{\infty}G_{pk}(\Omega)\frac{Z_k(\Omega)/k}{Z_{\mathrm{norm}}}\tilde{\lambda}_k(\Omega), \tag{5}$$

which we refer to as the Lebedev equation. Here, ζ is the dimensionless *intensity* parameter,

$$\zeta = -\frac{qN_p h^2\omega_0 Z_{\mathrm{norm}}}{V_0\cos\phi_{s0}}, \tag{6}$$

Z_{norm} is the impedance normalization factor in units of Ohms, which can be arbitrarily chosen (see also Table 1). The

* ivan.karpov@cern.ch

END-TO-END LONGITUDINAL SIMULATIONS IN THE CERN PS

A. Lasheen*, H. Damerau, K. Iliakis, CERN, Geneva, Switzerland

Abstract

In the context of the LHC Injector Upgrade (LIU) project, the main longitudinal limitations in the CERN PS are coupled bunch instabilities and uncontrolled emittance blow-up leading to losses at injection into the downstream accelerator, the SPS. To complement beam measurements, particle tracking simulations are an important tool to study these limitations. However, to avoid excessive runtime, simulations are usually targeting only a fraction of the cycle assuming that bunches are initially matched to the RF bucket. This ignores all initial perturbations that could seed an instability. Simulations were therefore performed along the full PS cycle by using the BLonD tracking code optimized with advanced parallelization schemes. They include beam manipulations with several RF harmonics (batch compression, merging, splittings), controlled emittance blow-up, a model of the beam coupling impedance covering a wide frequency range, as well as beam and cavity feedbacks. A large number of macroparticles is required as well as arrays to store beam induced voltage spanning several revolutions to account for long range wakefields.

INTRODUCTION

The main target of the High Luminosity (HL)-LHC project is to increase the luminosity for collisions by an order of magnitude [1]. This objective relies on an increased beam brightness from the injectors, which were upgraded in the framework of the LHC Injector Upgrade (LIU) project [2]. The beam intensity shall be doubled. However, at high beam current, limitations arise due to collective effects such as beam instabilities or uncontrolled emittance blow-up.

In the PS, the two main longitudinal limitations to reach the target of $N_b = 2.6 \times 10^{11}$ protons per bunch (p/b) at extraction are coupled bunch instabilities along the ramp (dipolar and quadrupolar) as well as uncontrolled longitudinal emittance blow-up due to high frequency cavity impedance [3, 4]. The longitudinal emittance should be kept at the nominal value of $\varepsilon_l = 0.35$ eVs at extraction to fit in the rf bucket of the SPS, the final stage in the LHC injector chain. Therefore, extensive studies were conducted to find means to mitigate beam instabilities.

An essential tool for beam instability studies are macroparticle simulations. Previously the simulations were done targeting only a specific instance in the cycle to keep the runtime reasonable (hours to couple of days). An example is the study of dipolar coupled bunch instabilities where simulations were initially performed at constant beam energy [5]. The initial particle distribution then needs to be assumed as matched to the initial RF bucket or with an arbitrary mismatch. In reality mismatches accumulate all along the

_____
* alexandre.lasheen@cern.ch

cycle and can seed the onset of an instability. They should therefore be taken into account to better reproduce the instability threshold. For example, coupled bunch instabilities start after transition crossing where an initial perturbation is expected, while simulations were originally started with matched conditions during the ramp.

Several studies could benefit from tracking simulations covering a complete cycle. An example is the operation with a higher harmonic RF cavity as Landau RF system to damp instabilities [6]. The present option consists of using the narrow-band 40 MHz cavity along the ramp. However, due to the limited bandwidth of the system, the complete acceleration ramp cannot be covered in such an operation mode. Tracking simulations covering the whole ramp, including transition crossing, were hence needed to evaluate the necessity of a dedicated Landau RF system.

Another aspect is the generation of particles at large amplitude in the longitudinal phase space (referred to as "longitudinal halo"), beyond the 0.35 eVs amplitude at extraction which are lost at SPS injection. The generation of halo can occur at several stages during the cycle and may accumulate. The optimization of the bunch rotation prior to extraction then requires a good knowledge of the halo. A simulation covering the whole cycle is needed to evaluate the impact of each stage in the cycle in terms of halo generation.

In this paper, the particle tracking code BLonD was extended in order to take into account several aspects such as a dynamic beam coupling impedance model, the influence of feedback systems, as well as a complete representation of the cycle including all processes and RF manipulations. The simulation is then compared to measurements. Finally, the computing performances are detailed.

MODELING THE COMPLETE ACCELERATION CYCLE

Beams with various longitudinal parameters can be generated in the PS. In the context of this paper, the so-called BCMS-type beam (Batch Compression Merging Splitting) produced for the LHC is considered [7]. The complete momentum and RF voltage programs are shown in Fig. 1. In this configuration, 8 bunches are injected from the PS Booster in two consecutive injections spaced by 1.2 s. The beam is then accelerated to an intermediate energy plateau where RF manipulations are performed. The beam is thereafter accelerated to the top energy, passing through transition crossing. The beam is then split again four times and non-adiabatically shortened before extraction to fit in the 5 ns SPS RF bucket (bunch rotation). Along the cycle, the longitudinal emittance is adjusted by applying controlled blow-up [8].

The complete program was simulated using the BLonD tracking code [9] including all the RF manipulations and controlled blow-ups, with the same voltage programs as

INJECTION CHICANE BETA-BEATING CORRECTION FOR ENHANCING THE BRIGHTNESS OF THE CERN PSB BEAMS

T. Prebibaj*[1], S. Albright, F. Antoniou, F. Asvesta, H. Bartosik,
C. Bracco, G. P. Di Giovanni, E.H. Maclean, B. Mikulec, E. Renner[2]
CERN, Geneva, Switzerland
[1]also at Goethe University, Frankfurt, Germany, [2]also at TU Wien, Vienna, Austria

Abstract

In the context of the LHC Injectors Upgrade Project (LIU), the Proton Synchrotron Booster (PSB) developed an H⁻ charge exchange injection system. The four short rectangular dipoles of the injection chicane induce focusing errors through edge focusing and eddy currents. These errors excite the half-integer resonance $2Q_y = 9$ and cause a dynamically changing beta-beating in the first milliseconds after injection. Using the beta-beating at the positions of two individually powered quadrupoles, measured with k-modulation, correction functions based on a model response matrix have been calculated and applied. Minimizing the beta-beating at injection allows the machine to be operated with betatron tunes closer to the half-integer resonance and therefore with larger space charge tune spreads. In this contribution the results of the beta-beating compensation studies and the impact on the achievable beam brightness limit of the machine are presented.

INTRODUCTION

The LHC Injectors recently underwent major upgrades, as part of the LHC Injectors Upgrade (LIU) project [1], with the aim of achieving the high-intensity and high-brightness beams required by the High Luminosity LHC [2]. As part of these upgrades, the PS Booster (PSB) received a new charge exchange injection region, for converting the negative hydrogen ions (H⁻) from Linac4 [3] to protons, at injection.

The main limitation for the beam brightness achievable at the PSB are space charge effects at injection [4]. The Linac4 delivers H⁻ at an increased energy of 160 MeV, compared to its predecessor, Linac2, which delivered protons at an energy of 50 MeV. The increase of the PSB injection energy mitigates the space charge effects and allows the beam intensity to be doubled while having similar space charge detuning for the same transverse emittances.

The new PSB charge-exchange injection system [5] consists of a horizontal chicane and a thin carbon stripping foil. A set of four, short, pulsed, dipole chicane magnets (BSWs), creating a maximum horizontal bump of 46 mm, have been installed in a short 2.6 m straight section, located at the first sector of the machine, for each of the four PSB rings (16 independently powered magnets in total). The edge focusing of the rectangular BSWs causes quadrupolar field perturbations in the vertical plane. Furthermore, during the ramp-down of the injection chicane, eddy currents are generated in the

metallic vacuum chamber, which distort the magnetic field seen by the beam. The eddy currents induce a sextupolar field, proportional to the ramp rate of the BSWs [6]. Since the beam enters the magnets with an offset with respect to the center of the BSWs, the sextupolar component leads to feed-down quadrupolar field perturbations. All these focusing errors cause distortion of the vertical β function around the machine.

At injection, the incoherent space charge tune spread can reach values up to $\Delta Q = -0.5$ [7]. The systematic resonances at the integer tunes $4Q_{x,y} = 16$ are strongly excited by the space charge potential due the lattice periodicity of 16, in combination with all other random field errors. To avoid beam degradation due to the integer resonances, the machine is operated very close to the vertical half-integer resonance $2Q_y = 9$. Operation with working points close to the half-integer resonance strongly enhances the β function distortions, which can eventually lead to beam losses. Studies showed that two of the main defocusing quadrupoles of the machine (QDE3 and QDE14) are optimal for compensating the perturbations caused by the injection chicane and for this reason they have been equipped with additional, individually controlled power supplies [8].

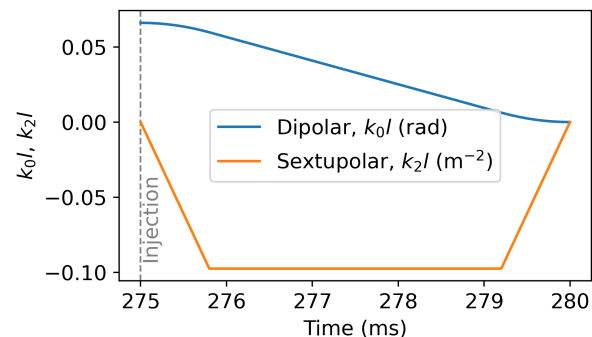## SIMULATIONS OF THE PSB INJECTION CHICANE OPTICS PERTURBATIONS

Figure 1: Modelled dipolar (blue) and sextupolar (orange) component of the BSWs.

The edge effects and the sextupolar components generated by eddy currents have been modelled in MAD-X [9] and applied in the PSB lattice. Figure 1 shows the expected dipolar and sextupolar component at one of the BSW magnets. The

* tirsi.prebibaj@cern.ch

OPTIMISED TRANSVERSE PAINTING SCHEMES FOR THE NEW 160 MeV H− INJECTION SYSTEM AT CERN

E. Renner*[1], S. Albright, F. Antoniou, F. Asvesta, H. Bartosik,
C. Bracco, G. P. Di Giovanni, B. Mikulec, T. Prebibaj[2],
F. M. Velotti, CERN, Geneva, Switzerland
[1]also at TU Wien, Vienna, Austria
[2]also at Goethe University, Frankfurt, Germany

Abstract

A major aspect of the LHC Injectors Upgrade (LIU) project at CERN is the Proton Synchrotron Booster (PSB) connection to the newly built Linac4 and the related installation of a new 160 MeV H− charge exchange injection. This contribution presents the first operational experience with the new injection system and its flexibility of applying horizontal phase space painting to tailor different beams to the respective user-defined brightness targets. The presented measurement and multi-particle simulation results focus on the optimisation of the required transverse injection settings to reduce losses when producing high-intensity beams, i.e. for the ISOLDE experiment. In this context, feasibility studies towards applying numerical optimisation algorithms for improving and efficiently adapting the respective injection settings online are presented.

INTRODUCTION

The PSB is the first synchrotron in the CERN injector complex and consists of four superposed rings. It was upgraded during the Long Shutdown 2 (LS2) in 2019/2020 as part of the LIU project [1], with the aim of doubling the beam brightness for the High Luminosity LHC [2] era. When connecting the new 160 MeV H− accelerator Linac4 [3] to the PSB, the injection energy was increased from 50 to 160 MeV and with it the relativistic factor $\beta_r \gamma_r^2$ by a factor two. A key component of this connection is the newly installed charge exchange injection system [4], which replaces a conventional proton multi-turn injection. The injection process into the PSB is used for tailoring the wide range of transverse beam characteristics as requested by the various users at CERN, covering intensities from $N_{p_+} = \mathcal{O}(10^{10})$ to $\mathcal{O}(10^{13})$ protons per ring and normalized transverse emittances from $\epsilon_{n,\mathrm{rms}} < 0.7$ μm (LHC-like beams) to $\approx 9-10$ μm (high intensity, e.g. for the ISOLDE [5] or nTOF [6] experiment). Prior to the upgrade, the production of the high intensity fixed target beams with $N_{p_+} = 0.8 - 1 \cdot 10^{13}$ p+ per ring resulted in up to $30 - 40\%$ losses at the injection septum due to the nature of the conventional multi-turn injection. With the new injection system, similar beams can be produced while keeping the losses within a few percent.

The required transverse beam characteristics for each user are customized by defining the programmable field decay of the horizontal injection bump as well as the offset between injected beam and circulating beam orbit during the injec-

tion process. This tailoring of the phase space distribution during injection is referred to as phase-space painting and enables a reduction of the charge density during beam accumulation, particularly when injecting high intensity beams. Consequently, the space charge detuning is reduced and emittance growth due to interaction of the detuned protons with integer resonances mitigated. Adequate painting schemes to produce operational beams with the same parameters as before the upgrade (pre-LS2) were previously defined using multi-particle simulations [1, 7–9]. These have been refined with beam and are now successfully used in operation. However, automatically optimising these programmed transverse painting schemes based on pulse per pulse modulation user requests and beam instrumentation feedback becomes a key aspect to improve operational efficiency, especially considering the perspective of increasing the delivered intensity for selected fixed target beams to $I > 1 \cdot 10^{13}$ p+ per ring.

This contribution presents simulation and measurement results to assess the impact of applied transverse painting settings on the losses obtained during high intensity beam production, taking an ISOLDE-like beam as an example. Subsequently, we discuss the potential of applying numerical optimisation algorithms to set and adapt the transverse painting functions automatically.

PSB CHARGE EXCHANGE INJECTION AND PAINTING SETTINGS

The Linac4 H− beam features normalised transverse emittances $\epsilon_{u,n} \approx 0.3$ μm in both planes $u = x, y$. Beam can be accumulated in the PSB over up to $n_t = 150$ turns, which corresponds to an injection over $t_{\mathrm{INJ}} = 150$ μs considering the PSB revolution period at injection energy $\tau \approx 1$ μs. For the here presented high intensity beam production studies, a chopping factor of $CF = 0.6$ is applied to the H− beam. This results in an injected intensity of $I_{\mathrm{INJ/turn}} \approx 1 \cdot 10^{11}$ p+ per PSB turn of beam accumulation [9], based on the present Linac4 peak current of 26 mA. The PSB accelerates beam from 160 MeV to 2 GeV in 530 ms with a 1.2 s repetition rate. In this contribution, we use time in ms relative to the start of the cycle ("C-time") to refer to time instances. Injection takes place at C275, extraction at C805.

The new injection system is illustrated in Fig. 1. The H− beam coming from Linac4 (red in Fig. 1) is injected via a ≈ 200 μg cm−2 carbon stripping foil [10–13]. The already circulating beam (blue in Fig. 1) is horizontally deflected towards the foil by a chicane in the injection region [14],

* elisabeth.renner@cern.ch

SPACE CHARGE RESONANCE ANALYSIS AT THE INTEGER TUNE FOR THE CERN PS

F. Asvesta and F. Schmidt, CERN, Geneva, Switzerland

Abstract

In the context of the LHC Injectors Upgrade (LIU) project, a series of studies have been performed in order to better understand the beam brightness limitations imposed by resonances and space charge effects.

Space charge simulations using the adaptive space charge solver as implemented in the MAD-X code conducted for the CERN Proton Synchrotron (PS) show that a particle approaching the integer tune of Qx = 6 demonstrates a resonant behavior. The analysis of the single particle transverse motion reveals the excitation of a second order resonance. The interplay of the space charge effect and the optics perturbation in the regime of the integer tune on this excitation was further investigated. The simulations were complemented with the analysis of the resonance driving terms coming from the space charge potential derived in a classical perturbative approach.

INTRODUCTION

The space charge is a dominant effect in high brightness low energy machines like the CERN PS. In this respect, multiple studies were conducted in order to understand the limitations for pushing the brightness in the scope of the LHC Injectors Upgrade (LIU) project [1]. Numerous studies, have shown that the available tune space in the PS is limited by both machine error and space charge driven resonances [2–6]. With such a limited transverse tune space, there is a need to better understand the impact of the integer resonance on the beam and investigate the sources of the excitation [7].

Experimental and simulation studies have been performed at the CERN PS to understand space charge effects in conjunction with sextupole non-linearities [3], including tune working points that sample a sextupole resonance but also the integer resonance. The minimum horizontal bare machine tune used in experiments and simulations alike was $Q_x = 6.039$, i.e. slightly above the integer while the maximum horizontal incoherent tune spread was -0.05. For the simulations discussed in this paper the code used is MADX-SC, an extension of the MAD-X Ref. [8] code including a space charge (SC) implementation of the adaptive mode. MADX-SC is presented in more details in Ref. [9] at this workshop.

For the SC studies presented here, the MADX-SC adaptive mode was selected, in which the beam emittances are re-calculated from the particle distribution at each turn in order to adapt the SC kicks accordingly. The analytical solvers allow simulating just a few 1'000 macro-particles and is therefore the only way to reach long periods, e.g. 500'000 turns for the typical CERN PS storage time. However, the SC force recalculations of the adaptive mode introduces some noise to the beam that needs to be minimized by increasing the number of macro-particles. For the PS simulation we had to increase the number of macro-particles from 1'000 to 2'000 to reduce the noise to an acceptable level [9]. This has to be seen as a compromise between simulation speed and artificial emittance blow-up, although this is much less of a problem than for the Particle In Cell (PIC) simulations [10–12]. It should be noted that MADX-SC also has a self-consistent mode but its much larger noise levels and longer simulation times make it impractical for most applications.

The simulation results will be discussed taking into account the PS complexity concerning matching of the tunes. The PS is a machine with combined function magnets with additional circuits for Pole Face Windings (PFWs). The combined function magnets define the transverse tune space that is accessible for the PS while the PFWs and additional quadrupoles, namely the Low Energy Quadrupoles (LEQs), can be used for fine adjustment of the tunes. The perturbations of the optics, when different combinations of the above elements are used, have an impact on resonance excitation in the presence of the space charge force.

In the first section, the analysis of the resonance structure found in phase space during the simulations will be presented. In the second section, the nature of the excitation of this higher order resonance on the integer tune will be discussed using the calculation of the resonance driving terms coming from the space charge potential and the harmonic analysis of the beam size and hence the beta functions as the integer resonance is approached.

RESONANCE ISLANDS IN SIMULATIONS

MADX-SC simulations are conducted for a working point close to the integer tune, $Q_x = 6.039$ and $Q_y = 6.479$ with the beam parameters shown in Table 1. To this end, a particle distribution of 2'000 macro particles is chosen to minimize numerical noise. A single particle that basically sits in the center of the bunch with very small initial coordinates is added to the 2'000 particle distribution. This special particle can be considered as a probe particle that is influenced by the full beam but itself affects very little the other particles of the bunch. Therefore, this particle is very close to the closed orbit and can be used to determine the maximum SC tune shift by analyzing its turn-by-turn motion.

Tune Matching as in the Experiment

In this section we are using the PFW for a large shift of the working point from the base tunes. The fine-tuning towards the horizontal integer and the vertical half integer

3D SYMPLECTIC SPACE CHARGE IMPLEMENTATION IN THE LATEST MAD-X VERSION

A. Latina, F. Schmidt, H. Renshall, CERN, Geneva, Switzerland,
Y. Alexahin, FNAL, Batavia, USA

Abstract

In 2018 as part of a collaboration between CERN and FNAL, the space charge (SC) implementation has been upgraded in a test version of MAD-X. The goal has been to implement the 3D symplectic SC kick together with a number of new features and benchmark it with earlier MADX-SC versions. Emphasis was given to the use of the Sigma Matrix approach that allows to extend MAD-X optics calculations.

In the meantime, significant effort has been made to fully debug and optimize the code and in particular to achieve a speed-up of the simulations by a factor of 2. The code has been ported to the latest MAD-X version, the elaborated set-up procedures have been automated and a user manual has been written.

INTRODUCTION

In 2010 (see Ref. [1]) V. Kapin and Y. Alexahin from FNAL started to implement the frozen space charge model into MAD-X [2]. One of the authors, F. Schmidt, joined their effort in 2012, establishing a special Fermilab version that we call MADX-SC, that has been presented in Ref. [3]. In the meantime, we have made a thorough cleaning and debugging of the code and have ported it to the latest MAD-X version. A manual has also been provided [4].

MADX-SC features both the frozen SC mode (as requested by BNL [5]) and the adaptive SC mode, the latter means that the SC force is recalculated when the emittances or beam intensity are changing. One can consider this as somewhere in between frozen and the full self-consistent mode, the latter provided in SC Particle-In-Cell (PIC) codes like Py-Orbit [6]. The adaptive mode allows for SC simulations with a few 1,000 macro-particles, and is therefore very fast and the only way to reach long periods, e.g., 500,000 turns for typical CERN PS SC runs. However, these SC force recalculations introduce some noise to the beam that needs to be minimized by increasing the number of macro-particles. For the PS simulation we had to increase the number of macro-particles from 1,000 to 2,000 to reduce the noise to an acceptable level. Nevertheless, this has to be seen as a compromise between simulation speed and artificial emittance growth due to numerical noise, although this is much less of a problem than for the PIC simulations.

This report discusses the physics aspects of MADX-SC in the first chapter, and summarizes the latest code development in the second chapter.

THE PHYSICS OF THE MADX-SC IMPLEMENTATION

Symplectic 3D SC Kick

We will concentrate here on the main MADX-SC design principles, further details can be found in Ref. [3].

The SC kick will be automatically symplectic if it is derived from a potential. We assume the bunch charge density to be of the form

$$\rho(x, y, z, t) = \frac{\lambda(z - v_0 t)}{2\pi \sigma_x \sigma_y} \exp\left(-\frac{x^2}{2\sigma_x^2} - \frac{y^2}{2\sigma_y^2}\right), \quad (1)$$

with λ being the line charge density, which should not be necessarily Gaussian but the present implementation is limited to a Gaussian profile.

For a long bunch, $\sigma_z \gg \max(\sigma_x, \sigma_y)$, the space-charge potential can be factorized in a similar fashion

$$\phi(x, y, z, t) \cong \lambda(z - v_0 t) \cdot \Phi(x, y), \quad (2)$$

where the two-dimensional potential function Φ can be presented in the form [7] [1]

$$\Phi(x, y) = \int_0^1 \left\{ \exp\left(-\frac{x^2 t}{2\sigma_x^2} - \frac{y^2 r^2 t}{2\sigma_y^2[1 + (r^2 - 1)t]}\right) - 1 \right\} \frac{dt}{t\sqrt{1 + (r^2 - 1)t}}, \quad (3)$$

with $r = \frac{\sigma_y}{\sigma_x}$ for $\sigma_y < \sigma_x$. If $\sigma_y > \sigma_x$ one can use formulas with interchanged x and y. Computing all components of a quasi-stationary Maxwellian field from the same potential ensures the symplecticity of the associated kick.

The potential in Eq. (3) is regularized and satisfies the boundary condition

$$\Phi(x, y)|_{x=y=0} = 0. \quad (4)$$

As a future development it can be complemented with a longitudinal wake which is independent of the transverse position (in order not to break the symplecticity).

Note [7] discusses the derivation of Eq. (3) in detail and considers methods of its numerical calculation in cases of small, large, and intermediate values of the transverse displacement, in units of beam sizes. Report [8] presents precision tests for each of these cases.

---

[1] Gaussian units are used. To convert to SI units the r.h.s. should be divided by $4\pi\varepsilon_0$

A DEDICATED WAKE-BUILDING FEEDBACK SYSTEM TO STUDY SINGLE BUNCH INSTABILITIES IN THE PRESENCE OF STRONG SPACE CHARGE

R. Ainsworth*, A. Burov, N. Eddy, A. Semenov, Fermilab†, Batavia, USA

Abstract

Recent advances in the theoretical understanding of beam stability in the presence of strong space charge, has suggested a new class of instabilities known as convective instabilities. A novel approach to excite and study these instabilities will be to install a 'waker' system, a dedicated wake-building feedback system. The System was installed in the Fermilab Recycler and commissioned during 2021. The first results are presented.

INTRODUCTION

The transverse mode coupling instability (TMCI) is known to be one of the main intensity limitations for bunch stability in circular machines. For many years, space charge was thought to have a stabilizing effect on TMCI raising the instability threshold to higher intensities. However, recent advances in the theoretical understanding of beam stability in the presence of strong space charge has led to the suggestion of a new class of instabilities, convective instabilities [1–4]. Numerical simulations [5] taking into account space charge also see these instabilities. It is believed these instabilities have been observed [6, 7] before but are often attributed to TMCI.

In order to study these instabilities, a new experimental program making use of Fermilab's existing accelerator complex is underway. The primary objective of the proposed research will be to characterize these instabilities in the presence of varying space charge and varying wake amplitudes. Usually, the wake amplitudes which drive instabilities are machine dependent and are determined by the impedance of the components installed within the machine. A novel approach to control instabilities will be to install a 'waker' system, a dedicated wake-building feedback system.

WAKER CONCEPT

One of the advantages of simulations, is that the user can vary the wake parameter however they please. If this could be accomplished in actual machine, it would open the door to many exciting studies that could not normally be performed. The waker system is a novel concept which tries to mimic this approach and allow the user to define their own wake.

The system design will be similar to a traditional damper system however, used to excite instabilities rather than damp them. The concept of the system is as follows;

* The user defines a wake, W(s).

* The system will measure the position and intensity of the bunch at different time slices along the bunch in a single turn given by x_j and q_j respectively.

* On the next turn, the system applies multiple kicks along the bunch where the kick size, K is determined by the convolution of transverse offsets of the upstream time slices with the wake function of the longitudinal position difference

$$K_i \propto \sum_{j=1}^{i-1} x_j q_j W(s_j - s_i) \tag{1}$$

The bandwidth of the system should be much bigger than the inverse bunch length i.e.

$$\Delta\omega >> 1/\sigma_b \tag{2}$$

For standard operation in the Recycler, the beam is bunched at 53 MHz. A typical bunch length is 2 ns, which would require a bandwidth larger than 500 MHz which would not be feasible to build. However, the beam can be re-bunched to 2.5 MHz which is routinely performed for the Muon program. In this case, a typical 1-sigma bunch length of 30 ns can be expected and so, a bandwidth larger than 30 MHz would be needed. Assuming a full bunch length equivalent to 4-sigma of 120 ns, a 100 MHz system would provide 12 time slices across the bunch and a 200 MHz system would provide 24 time slices. Based on this, the bandwidth of the system will be designed to be at least 100 MHz.

WAKER SYSTEM

The waker system is installed in the Fermilab Recycler. The main components are as follows:

Kicker A 0.5m vertical stripline kicker is used to provide the kicks that mimic a wakefield. The length is chosen based on the frequency response in order to meet a bandwidth of 200 MHz.

Pickups Two split plate BPMs are used. Ideally, the two BPMs would be separated by 90° in betatron phase advance. The two signals from these BPMs can be combined with the correct coefficients to control the phase to the kicker. The pickups used are located at 206 and 208 in the Recycler and are separated in phase by 82°.

---
* rainswor@fnal.gov
† Operated by Fermi Research Alliance, LLC under Contract No. De-AC02-07CH11359 with the United States Department of Energy.

COUPLED BUNCH INSTABILITIES GROWTH IN THE FERMILAB BOOSTER DURING ACCELERATION CYCLE*

C. M. Bhat[†] and N. Eddy, Fermilab, Batavia, IL, U.S.A.

Abstract

Currently, Fermilab Booster accelerates $\sim 4.5 \cdot 10^{12}$ protons per pulse (ppp) in 81 bunches from 400 MeV to 8 GeV at 15 Hz to provide beam to multiple HEP experiments and is being upgraded to handle higher beam intensity $> 6.7 \cdot 10^{12}$ ppp at a repetition rate of 20 Hz. In the current mode of operation, we control longitudinal coupled bunch instabilities (LCBI) using combination of passive and active dampers. The issues with LCBI are expected to worsen at higher beam intensities. Here, we would like to investigate at what time in the beam cycle a particular mode is going to originate and how much it contributes at a different time of the acceleration cycle using the collected wall current monitor data from injection to extraction. Also, measure growth rates as a function of beam intensity for some dominant modes. Finally, this paper presents results from the observed LCBI analysis for the highest available beam intensities, unexpected findings, and future plans to mitigate the LCBI at higher beam intensities.

INTRODUCTION

The Fermilab Booster is one of the oldest RCS in the world which cycles at 15 Hz rate [1-3] and providing 8 GeV beam to HEP programs for the last 50 years. Until 2016 the beam in the Booster was accelerated with low duty factor, e.g., during the early part of the Main Ring fixed target HEP era it provided $\sim 2 \cdot 10^{12}$ ppp with an average repetition rate slightly more than 0.5 Hz out of 15 Hz and with lower beam brightness. In early 1980s, as we entered the collider era along with fixed target HEP programs, the demand on the beam intensity from the Booster per cycle as well as the beam delivery repetition rate increased. All these periods, the longitudinal coupled bunch instability was troublesome in the Booster and, was being addressed and controlled [4-13]. In 2012, Fermilab entered the intensity frontier era PIP [14, 15] and by the end of this decade it will be in PIP-II era [16]. Currently, we are providing $> 4.3 \cdot 10^{12}$ ppp at 15 Hz rate from the Booster and, >700 kW proton beam power on the NuMI neutrino target and at the same time beam to multiple Booster neutrino experiments. Between now and when the PIP-II comes online, we have a near-term goal to increase the beam output power per Booster cycle by about 25%. PIP-II calls for a further increase in beam intensity by $\sim 50\%$ and a cycle rate of 20 Hz. In this regard the coupled bunch instability needs to be revisited

Since the start of the Booster, the beam has been injected into the Booster without any RF buckets opened. After the

completion of the injection the beam is captured slowly in the RF buckets with harmonic number h=84. So, it is expected that the bunches are well matched to the RF buckets from the start of their formation with minimal longitudinal instabilities. However, during the acceleration from injection energy to 8 GeV beam encounters transition crossing at γ=5.47 with normal transition phase jump and we have observed significant longitudinal emittance growth only after transition energy. This emittance growth is related to longitudinal coupled bunch instability observed after transition crossing [7]. Since then, multiple upgrades were made to add passive [8] and active [4, 9, 11-13] dampers to mitigate LCBI in the beam. In all these cases it was enough to enable the active dampers only after the transition crossing and monitor the coupled bunch instability in the extracted beam using a wall current monitor (WCM) in the 8 GeV transfer line. During PIP-II era, 800 MeV beam will be injected directly into the Booster RF buckets and by the end of the injection process the beam distribution is expected to match well with the RF buckets. Nevertheless, the bunch intensity will be significantly higher than that in the current operation. As a result of this, it is of interest to investigate the evolution of LCBI in Booster for high intensity beam, ahead of PIP-II and develop mitigation strategy.

ASPECTS OF DIPOLE LCBI

Theory of longitudinal coupled bunch instability and stability criterion are one of the widely discussed subjects in beam physics [17-20]. An application of the theory to study and control the coupled bunch dipole mode instability in the Fermilab Booster was carried out by D.P. McGinnis [4, 5] in early 1990s. Here, we highlight some key aspects of the theory in the context of studies carried out for the intensity upgrade in the Booster.

Circulating bunches of charged particle in a synchrotron give rise to longitudinal as well as transverse wake fields because of machine impedance including higher-order modes of RF cavities. The longitudinal wake field which is not decayed between arrival of consecutive bunches in the ring will be responsible for longitudinal coupling between bunches and is an important source of instability in longitudinal plane. The wake fields can potentially cause both bunch displacement as well as distortion and help growing exponentially during successive passage in the synchrotron. The particles in bunches execute synchrotron oscillations due to RF force. So, the displaced bunches will also experience this additional force in the RF bucket which adds up for further emittance dilution and possibly beam loss during the beam acceleration. There are other sources of bunch oscillations which may not be due to wake field effects. Such exam-

STATUS OF LAYOUT STUDIES FOR FIXED-TARGET EXPERIMENTS IN ALICE BASED ON CRYSTAL-ASSISTED HALO SPLITTING*

M. Patecki†, D. Kikoła, Warsaw University of Technology, Faculty of Physics, Warsaw, Poland
A. Fomin, D. Mirarchi, S. Redaelli, CERN, Geneva, Switzerland

Abstract

The Large Hadron Collider (LHC) at the European Organization for Nuclear Research (CERN) is the world largest and most powerful particle accelerator colliding beams of protons and lead ions at energies up to 7 TeV and 2.76 TeV, respectively. ALICE is one of the detector experiments optimised for heavy-ion collisions. A fixed-target experiment in ALICE is considered to collide a portion of the beam halo split by means of a bent crystal with an internal target placed a few meters upstream of the detector. Fixed-target collisions offer many physics opportunities related to hadronic matter and the quark-gluon plasma to extend the research potential of the CERN accelerator complex. This paper summarises our progress in preparing the fixed-target layout consisting of crystal assemblies, a target and downstream absorbers. We discuss the conceptual integration of these elements within the LHC ring, impact on ring losses, conditions for a parasitic operation and expected performance in terms of particle flux on target.

INTRODUCTION

The ALICE fixed-target (ALICE-FT) programme [1] is proposed to extend the research potential of the Large Hadron Collider (LHC) [2] and the ALICE experiment [3]. The concept is based on steering onto a solid internal target a fraction of the proton beam halo split by means of a bent crystal, similar to crystals being developed for beam collimation at the LHC [4–6]. Splitting the beam is performed by exploiting the channeling process occurring inside a bent crystal, resulting in a trajectory deflection equivalent to the geometric bending angle of a crystal body [7]. Such a setup, installed in the proximity of the ALICE detector, would provide the most energetic proton beam ever in the fixed-target mode with centre-of-mass energy per nucleon-nucleon ($\sqrt{s_{NN}}$) of 115 GeV offering a possibility to study the hadronic matter and to provide inputs for cosmic ray physics as summarised by the AFTER@LHC study group [1, 8].

Our proposal of the ALICE-FT layout follows general guidelines on technical feasibility and impact on the LHC accelerator of potential fixed-target experiments provided by the LHC Fixed Target Working Group of the CERN Physics Beyond Colliders forum [9, 10]. We also profit from the preliminary designs reported in [11, 12] and from the design study of an analogous fixed target experiment at the LHC proposed to measure electric and magnetic dipole moments of short-lived baryons [13].

In this report, we summarise the status of the ALICE-FT layout, including conceptual integration of its elements (crystal and target assemblies, downstream absorbers), their impact on ring losses, and expected performance in terms of particle flux on target, taking into account parasitic and dedicated operation modes.

MACHINE CONFIGURATION

A potential installation of the ALICE-FT setup will coincide with a major LHC upgrade in terms of instantaneous luminosity, commonly referred to as the High-Luminosity LHC (HL-LHC) [14], taking place in the Long Shutdown 3 (2025-2027), to make it ready for Run4 starting in 2027. Some of the expected beam parameters, having a direct impact on the ALICE-FT experiment performance, are given in Table 1. Among beam parameters being a subject of the upgrade, we highlight the total beam current increase nearly by a factor of 2, up to about 1.1 A, leading to more than 0.7 GJ of total beam energy stored in the machine. A highly efficient collimation system is therefore present in the LHC [15] and it will be upgraded for the HL-LHC [16]. Its role is to intercept the beam halo and to protect the cryogenic aperture from beam losses as some tens of mJ/cm^3 deposited in a superconducting magnet can cause an abrupt loss of its superconducting properties, i.e. a magnet quench. The halo splitting scheme is to be embedded into the transverse hierarchy of the betatron collimation system, as shown in Fig. 1, such that the collimation system efficiency is not affected. A fraction of secondary halo particles redirected towards the target can be used for fixed-target collisions instead of disposing them at the absorbers. The present collimation system is organised in a precise multi-stage hierarchy (see Table 2) over two dedicated insertions (IRs): IR3 for momentum cleaning and IR7 for betatron cleaning. Each collimation insertion features a three-stage cleaning

Table 1: Some Parameters of the Future HL-LHC Beams Important for the ALICE-FT Experiment, Referred to as *Standard* in [14]

Beam energy in collision	E	7 TeV
Bunch population	N_b	$2.2 \cdot 10^{11}$
Maximum number of bunches	n_b	2760
Beam current	I	1.09 A
Transverse normalised emittance	ε_n	2.5 µm
β^* at IP2		10 m
Beam crossing angle at IP2		200 µrad

DESIGN AND IMPLEMENTATION OF
FAST MACHINE PROTECTION SYSTEM FOR CSNS

P. Zhu[*1], D. P. Jin[1], Y. L. Zhang[1], Y. C. He[1], K. J. Xue[1], X. Wu[1], L. Wang[1]

Institute of High Energy Physics, Chinese Academy of Sciences, Beijing, China

[1]also at Spallation Neutron Source Science Center, Dongguan, China

Abstract

According to the design concept of high availability, high reliability and high maintainability, CSNS accelerator fast machine protection system (FPS) adopts the distributed architecture based on "high-performance chip (FPGA) + high-speed transmission link (Rocket I/O) + VME". We self-developed the main logic board with the function of reading and writing via VME, and which is the core and real-time to summary each interlocking signals, then determine and send out the protection action with accurately and stably. Simultaneously, in order to achieve interaction with each device flexible, we also self-customized a variety of interface boards. The permanent and instantaneous protection strategy was researched independently to meet the requirements of improving the efficiency of beam supply under the premise of ensuring operational safety. CSNS accelerator FPS has been put into operation for nearly six years stable and reliable until it is strict and systemic to test the function and performance on line, especially time-consuming, which is one of the important basic conditions for the efficient operation of CSNS accelerator.

INTRODUCTION

The Chinese Spallation Neutron Source (CSNS) is a large-scale scientific facility, which is mainly composed of an 80 MeV LINAC accelerator (LINAC), a 1.6 GeV Rapid Cycling Synchrotron (RCS), a target station, LINAC to Ring beam transport line (LRBT), RCS to target beam transport line (RTBT), multiple neutron scattering spectrometers and corresponding supporting facilities [1]. CSNS is the first pulsed neutron source facility in developing countries. It is expected to have positive effects in promoting the development of fundamental sciences and technology.

CSNS is based on accelerated high-energy protons, so if equipment failure or other reasons cause the high-energy protons to deviate from the normal orbit, the equipment along the beam, such as Drift Tube LINAC (DTL), may be suffered from graze or permanent damage by continuous beam bombardment because of the strong destructiveness protons. Therefore, it is essential to establish machine protection system to cut off the beam with high reliability in the shortest possible time, and execute the relevant progress in order time accurately. The CSNS accelerator fast machine protection system (FPS) is crucial to be need to meet the special functional requirements, which must have the characteristics of high stability, high reliability, and high speed

* zhup@ihep.ac.cn

under long-term operation. This article will introduce the requirements of system function, the design of architecture and protection strategy, and also the operation status.

REQUIREMENT

According to the simulations and calculations carefully, if beam abnormality occurs during LINAC accelerator operation, the entire protection action should be completed within 10 μs to cut off the beam promptly [2], as shown in Figure 1. Generally, the response time of PLC-based slow protection system (SPS) is on the level of milli-seconds [3], which cannot meet the requirements of the CSNS LINNAC accelerator. In view of the overall the urgent and actual requirements of the CSNS accelerator, we decided to design and develop a fast machine protection system (FPS) based on the current high-speed digital electronic technology, and the key purpose of design is to achieve the response time of less than 10 μs.
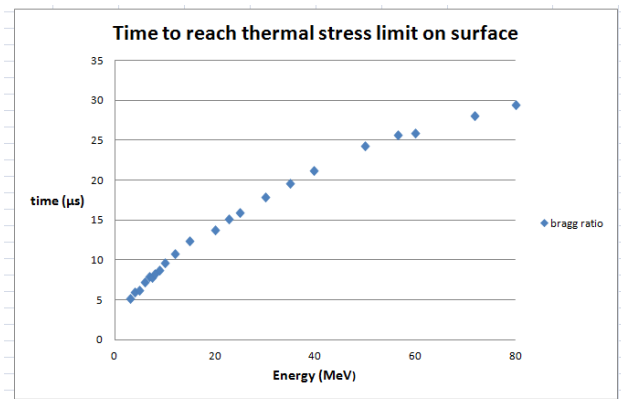

Figure 1: The relationship between the thermal stress limit in the material (copper) and the cumulative beam loss time. ① I=15 mA, $\sigma_x = \sigma_y = 0.2$ cm, J=62 J/gm (energy density); ② Un-chopped beam, 15 mA; ③ Beam size: 0.2 cm ×0.1 cm RMS; ④ Hitting the components directly.

ARCHITECTURE

According to CSNS accelerator physical design and beam research requirements, CSNS accelerator currently has a total of 6 beam targets [4], including: Ion Source (IS), LRBT Beam Dump (L-DUMP), LR Beam Dump (LRDUMP), Injection Beam Dump (I-DUMP), RTBT Beam Dump (R-DUMP) and target station, each beam target corresponds to the beam along the line and related equipment. Therefore, CSNS machine protection system needs to be able to timely

AN OPERATIONALLY INTEGRATED APPROACH TO THE SNS 2.8 MW POWER UPGRADE*

J. Galambos†, on behalf of the PPU team, SNS, Oak Ridge TN, USA

Abstract

The Spallation Neutron Source (SNS) accelerator consist of a 1 GeV H⁻ linac and an accumulator ring producing a 1.4 MW pulsed proton beam which drives a spallation neutron source [1]. The Proton Power Upgrade pro-ject will double the power capability from 1.4 to 2.8 MW by increasing the linac beam energy 30% and the beam current about 50%. Equipment upgrades include new superconducting RF cryomodules and supporting RF equipment, upgraded ring equipment, and upgraded high power target systems. An important aspect of the up-grade is a gradual power ramp-up starting in 2022 in which new equipment is installed during maintenance outages as it arrives, and used in subsequent run periods.

INTRODUCTION

The SNS is a neutron scattering materials science user facility that has been operating since 2006. The neutron flux used to study material structures and properties is proportional to the proton beam power, the history of which is shown in Fig. 1. Beam power has been operating stably at the design level of 1.4 MW since 2018, and SNS has been embarked on a Proton Power Upgrade (PPU) project since 2017 [2, 3]. This project aims to double the beam power capability by increasing the beam energy by 30% and increasing the average beam current by 50%. Of the post-upgrade 2.8 MW proton beam power capability, 2 MW will be provided to the existing First Target Station (STS) at SNS, and additional power will be available to power a new Second Target Station [4], which is a separate ongoing project. The PPU project received approval for long lead procurements in the areas of superconducting cryomodules, RF equipment and RF service building upgrades in the fall of 2019. In fall 2020 the project baseline and the start of construction was approved.

A major consideration of high-power proton accelerators is beam loss, which is discussed in section 2, along with some discussion on operational experience that guides the upgrade. The progress of different PPU technical systems is discussed in section 3. The coordination of the upgrade equipment installation and use with ongoing operations resulting in a gradual power ramp-up is discussed in section 4.

OPERATIONAL EXPERIENCE

As indicated in Fig. 1, SNS has been operating stably at 1.4 MW for 3 years. Accelerator availability of over 90% and

---

over 4500 operational hours per year have been sustained over this period. The operational experience garnered since 2006 guides the PPU upgrade choices for 2.8 MW operation [2, 3]. In addition to the equipment needed to provide the higher power, PPU will provide additional beam instrumentation and control in the injection dump area, which is presently has limited diagnostics.

Beam loss was a major consideration in the design of SNS. Beam loss was expected to be less than 1 W/m [5] (or <10⁻⁶ fractional loss for much of the facility) and this is the case. This level of beam loss is beyond what simulation tools accurately predict. But it is possible to scale anticipated post-upgrade beam loss from present observed beam loss levels at ~1 MW operation. This was done for the various sections of the SNS accelerator in Ref. [2], and the increase in beam loss and subsequent activation levels is expected to be smaller about a factor of 2 from presently observed residual activation levels. This increase can be accommodated without major impact on machine operations.
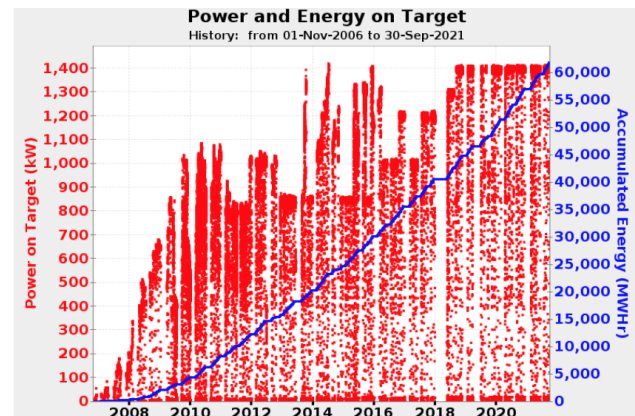

Figure 1: SNS Beam power history.

UPGRADE STATUS

Superconducting Linac

Seven new cryomodules will be installed in existing slots in the SNS high energy end of the linac [6]. Over the past year the superconducting RF cavities have been supplied by the vendor and cryomodule production is ramping up at the partner lab, JLab. Equipment procurements are largely in hand, cavities have been jacketed and qualified for the first 3 cryomodule strings, and the first cryomodule cold mass is nearing final assembly. (see Fig. 2). In addition, an 8th spare cryomodule has been added to the project scope. The cryomodule production is on schedule for delivery of the initial 2 cryomodules in April 2022.

SELF-CONSISTENT LONG-TERM DYNAMICS OF SPACE CHARGE DRIVEN RESONANCES IN 2D AND 3D

Ingo Hofmann and Adrian Oeftiger*
GSI Helmholtzzentrum für Schwerionenforschung GmbH, Darmstadt, Germany
Oliver Boine-Frankenheim, Technische Universität Darmstadt, Darmstadt, Germany

Abstract

Understanding the 3D collective long-term response of beams exposed to resonances is of theoretical interest and essential for advancing high intensity synchrotrons. This study of a hitherto unexplored beam dynamical regime is based on 2D and 3D self-consistent particle-in-cell simulations and on careful analysis using tune spectra and phase space. It shows that in Gaussian-like beams Landau damping suppresses all coherent parametric resonances, which are of higher than second order (the "envelope instability"). Our 3D results are obtained in an exemplary stopband, which includes the second order coherent parametric resonance and a fourth order structural resonance. They show that slow synchrotron oscillation plays a significant role. Moreover, for the early time evolution of emittance growth the interplay of incoherent and coherent resonance response matters, and differentiation between halo and different core regions is essential. In the long-term behaviour we identify a progressive, self-consistent drift of particles towards and across the resonance, which results in effective compression of the initial tune spectrum. However, no visible imprint of the coherent features is left over, which only control the picture during the first one or two synchrotron periods. An intensity limit criterion and an asymptotic formula for long-term rms emittance growth are suggested. Comparison with the commonly used non-self-consistent "frozen space charge" model shows that in 3D this approximation yields a fast and useful orientation, but it is a conservative estimate of the tolerable intensity.

INTRODUCTION

Beam intensity in operating or future high intensity circular hadron accelerators is limited by space charge effects on resonances [1]. Contrary to low intensity operation, where resonances are single particle phenomena, high intensity requires self-consistent treatment with differentiation between incoherent and coherent resonance effects as well as consideration of Landau damping of nonlinear coherent parametric resonances. Analytical or semi-analytical models of the latter do not exist – in contrast to the rich literature on impedance driven dipole modes –, hence we depend largely on simulation and careful theory-based interpretation.

Long-term space charge effects on synchrotron resonances have been measured in dedicated campaigns (see, for example, Refs. [1–3]). Comparison with simulation models is essential for understanding resonant processes and min-

imizing their effects on beam quality; but so far – for cpu and noise related reasons – only non-self-consistent "frozen space charge models" (FSM) have been employed in these campaigns, which require modeling of $10^5...10^6$ machine turns. Such fully self-consistent 3D simulations using large numbers of simulation particles and many turns of synchrotron lattices are quite possible. Examples are long-term studies of the Montague resonance with the IMPACT code [4], or recent work on parametric Landau damping using the SYNERGIA code [5].

Recently, coasting beam 2D studies in relatively short systems (hundreds of cells rather than hundreds of thousands) have been used as basis for conjectures on coherent resonance effects and suggestion of new types of synchrotron resonance charts based on assumed coherent shifts, with partly controversial conclusions (see Ref. [6], also Refs. [7, 8]). The need for *long-term* and self-consistent 3D studies to adequately address these issues becomes obvious.

Historically, Smith [9] first pointed out in the early 1960's that coherent effects on gradient error resonances should result in higher intensity; followed by Sacherer [10] who extended the concept of coherent shifts to nonlinear resonances in a 1D Vlasov-Poisson study. In the 1990's, the suggestion by Smith was partly confirmed in relatively short-term simulations by Machida [11]; a Vlasov model presented coherent frequencies in 2D including anisotropy [12], and a review article by Baartman [13] further advocated for the coherent shift concept. The distinction between coherent and incoherent second order resonance effects was studied experimentally in HIMAC [14] and the PSR [15].

In high intensity linear accelerators the theoretically predicted structural space charge resonance effects [16] got verified experimentally by detailed phase space diagnostics [17].

In circular accelerators space charge resonant effects are known to exist; however, distinguishing them from often dominating externally driven resonances and other machine specific effects continues to be a challenging issue for performance optimization of high intensity synchrotrons [18–21]. Besides studies in operating linear accelerators and synchrotrons, compact linear Paul trap devices are also used to explore – experimentally and theoretically – incoherent and coherent resonances in periodic focusing and 2D [22].

For high intensity hadron circular accelerators – different from linear devices – a main beam dynamics challenge is self-consistent and long-term 3D modelling including synchrotron oscillation, which has motivated the present study. As an exemplary case we choose a simple FODO cell for

_____

* a.oeftiger@gsi.de

IMPACT OF POWER SUPPLY RIPPLE ON THE BEAM PERFORMANCE OF THE LARGE HADRON COLLIDER AND THE HIGH-LUMINOSITY LHC *

S. Kostoglou†, H. Bartosik, Y. Papaphilippou, G. Sterbini, CERN, Geneva, Switzerland

Abstract

Harmonics of the mains frequency (50 Hz) have been systematically observed in the form of dipolar excitations in the transverse beam spectrum of the Large Hadron Collider (LHC) since the beginning of its operation. The power supply ripple, consisting of both fundamental and higher frequency components, is proven not to be the result of an artifact of the instrumentation systems with which they are observed. Potential sources of the perturbation have been identified through systematic analysis and experimental studies. Single-particle tracking simulations have been performed including a realistic power supply ripple spectrum, as acquired from experimental observations, to demonstrate the impact of such noise effects on beam performance.

INTRODUCTION

Since the start of the Large Hadron Collider (LHC) operation, harmonics of the mains power frequency (50 Hz) in the form of dipolar excitations have been perturbing the transverse beam spectrum. Similar observations of power supply ripple, including high-order harmonics, have also been reported in the past by several other accelerators such as the Relativistic Heavy Ion Collider (RHIC) and the Tevatron [1–4]. The presence of such perturbation may degrade the accelerator's performance by acting as an additional diffusion mechanism through the excitation of specific resonances. Together with the other resonances excited by the lattice non-linear fields and the beam-beam interactions, this effect can prove detrimental to the beam lifetime.

To this end, identifying the origin of the perturbation and applying mitigation measures is of paramount importance, especially for the High-Luminosity LHC (HL-LHC) era where a good understanding and control of all the beam degradation mechanisms is necessary, as unprecedented values of integrated luminosity are envisaged [5]. The present paper summarizes the main findings, which provide evidence that the 50 Hz harmonics correspond to real beam excitations rather than being an artifact of the instrumentation systems. It furthermore presents the dedicated experiments and measurements performed to identify their origin and illustrates the simulation analysis used to evaluate their impact on the beam lifetime. A thorough analysis of the 50 Hz harmonics in the LHC can be found in [6, 7].

OBSERVATIONS FROM THE LHC

The presence of a series of 50 Hz harmonics in the beam signal has been confirmed with measurements with several independent instruments. One of these instruments is the transverse Observation Box (ADTObsBox) which provides bunch-by-bunch and turn-by-turn calibrated position measurements [8–10]. The high-sampling rate allows the spectrum to be computed in a broad high-frequency range. Thanks to the calibrated metric of the turn-by-turn data used to compute the spectrum, the amplitude of each harmonic can be extracted.

Figure 1 shows the beam spectrum for the horizontal plane of Beam 2 as computed with the data obtained from the ADTObsBox for a frequency range up to 10 kHz. Two regimes of interest are identified: a cluster of 50 Hz harmonics extending up to 3.6 kHz (blue), referred to as the *low-frequency cluster*, and another regime with spectral components around 7-8 kHz (yellow), namely the *high-frequency cluster*. Based on the fact that the LHC revolution frequency, hence the sampling frequency, is not an exact multiple of 50 Hz (11.245 kHz), it can be seen that both clusters consist of 50 Hz harmonics and not aliases that could arise from the sampling of the data. Higher amplitudes of the harmonics in the high-frequency cluster are observed. Similar observations have been collected for both beams and planes.
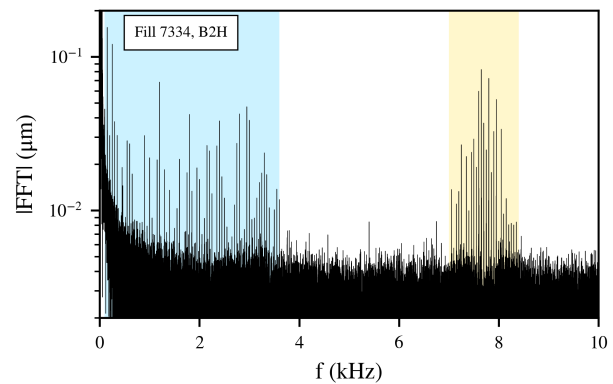

Figure 1: The horizontal spectrum of Beam 2 extending up to 10 kHz using the bunch-by-bunch and turn-by-turn data of the ADTObsBox. The low and high-frequency clusters, both consisting of 50 Hz harmonics, are illustrated with blue and yellow shaded areas, respectively.

Several observations confirm that the observed beam excitation is not an artifact of the instrumentation system. First, the harmonics are visible in several unrelated instruments and a comparison between the spectra before and after the

OPERATIONAL EXPERIENCE WITH NANOCRYSTALLINE INJECTION FOILS AT SNS

N.J. Evans*, Oak Ridge National Laboratory, Oak Ridge, USA

Abstract

The Spallation Neutron Source (SNS) uses 300-400 $\mu g/cm^2$ nanocrystalline diamond foils grown in-house at the Center for Nanophase Materials Sciences to facilitate charge exchange injection (CEI) from the 1 GeV H- linac into the 248 m circumference accumulation ring. These foils have performed exceptionally well with lifetimes of thousands of MW·hrs. This contribution shares some experience with the operation of these foils during 1.4 MW operation, and discusses current operational concerns including injection related losses, foil conditioning, deformation, and sublimation due to high temperatures. The implications for the SNS Proton Power Upgrade are also discussed.

INTRODUCTION

The Spallation Neutron Source is a 1.0 GeV short-pulse accelerator that operates at 60 Hz to produce an average power on target of 1.4 MW. Linac pulses are approximately 1 ms long, and are compressed by roughly a factor of 1000 in the accumulator ring. Injection into the ring is achieved via charge exchange injection using approximately 30x17mm, 300-400 $\mu g/cm^2$ thick nanocrystalline diamond foils grown on a Silicon substrate, a portion of which serves as a 'handle' for mounting. Figure 1 shows the various parts of the foil, including the conditioned corner on the bottom left. Foils are mounted at a 30° angle relative to injected and recirculating beams which increases the effective thickness determining stripping efficiency. The optimal foil thickness balances stripping efficiency, foil heating, beam scattering, and mechanical stability which can contribute to the stability of losses, and power to the injection dump. A foil changer mechanism, or 'chainsaw', allows the installation of up to 12 foils which are changed roughly once per year. In a typical year between 4 and 6 foils will be used and replaced, with one conditioned foil often left in to accommodate high-power target studies done immediately upon start up.

Early in the design of SNS the survivability of foils at the high average power of SNS operation was a major concern. Although there were problems with charge exchange injection at high power, the worst fears about foil failure have not been realized, and many issues discussed previously have been mitigated [1], [2]. After several years of routine operation at the SNS design power of 1.4 MW the foils have
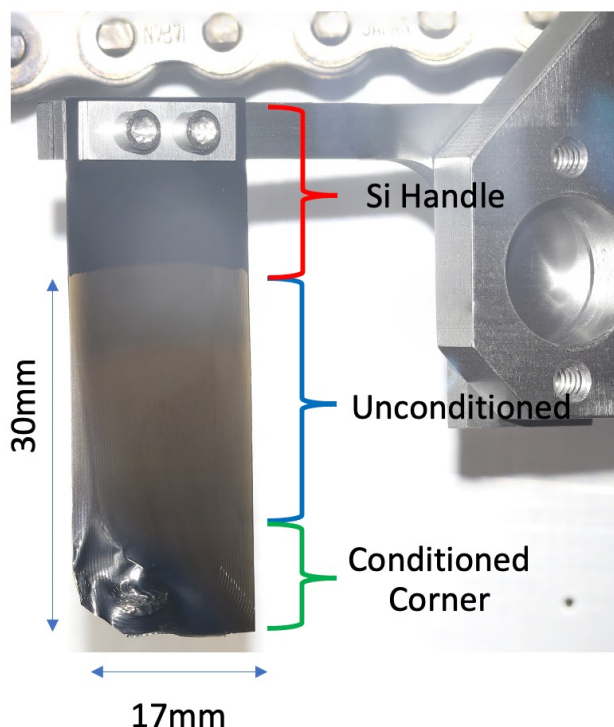
---
* nhe@ornl.gov

Figure 1: A used, mounted foil.

performed exceptionally well, with the best foils lasting an entire run cycle of 2500 MW·hrs or more.

The Proton Power Upgrade will increase the power capability of the SNS accelerator from 1.4 MW to 2.8 MW by increasing kinetic energy from 1.0 GeV to 1.3 GeV, and the charge per pulse from 24 μC to 33 μC by increasing the peak current in the linac. The 60 Hz repetition rate, and number of accumulated turns will remain the same. However, the actual power at which the accelerator will operate will be staged over several years as the First Target Station(FTS) will only be capable of handling 2.0 MW, with the remaining power eventually destined for the Second Target Station(STS). Key parameters affecting the foils are summarized in Table 1, where SNS refers to current operation, PPU/FTS the first stage of operation to the first target station after the completion of PPU, and STS the 2.8 MW era currently planned for the early 2030's. These upgrades have renewed interest in the limits of nanocrystalline foils for high power charge exchange injection.

Currently the primary challenges for operation are: beam loss, foil conditioning time, foil deformation, and foil sublimation. With the exception of foil sublimation, these are mainly an annoyance to operation, but do not represent single-point failures. Foil sublimation due to heating, how-

TEST OF MACHINE LEARNING AT THE CERN LINAC4

V. Kain*, N. Bruchon, S. Hirlander, N. Madysa,
I. Vojskovic, P. Skowronski, CERN, Geneva, Switzerland
G. Valentino, University of Malta, Msida, Malta

Abstract

The CERN H⁻ linear accelerator, LINAC4, served as a test bed for advanced algorithms during the CERN Long Shutdown 2 in the years 2019/20. One of the main goals was to show that reinforcement learning with all its benefits can be used as a replacement for numerical optimization and as a complement to classical control in the accelerator control context. Many of the algorithms used were prepared beforehand at the electron line of the AWAKE facility to make the best use of the limited time available at LINAC4. An overview of the algorithms and concepts tested at LINAC4 and AWAKE will be given and the results discussed.

INTRODUCTION AND MOTIVATION

The CERN accelerators generally use a modular control system to deal with the resulting complexity of hundreds or thousands of tuneable parameters. Low level hardware parameters are combined into higher level accelerator physics parameters defined by simulation results. For correction and tuning, low-level feedback systems are available, together with high-level physics algorithms to correct beam parameters based on observables from instrumentation. With this hierarchical approach large facilities like the LHC can be exploited efficiently.

There are still many processes at CERN's accelerators, however, that require additional control functionality. In the lower energy accelerators, models are often not available online or cannot be inverted to be used in algorithms. Sometimes instrumentation that could be used as input for model-based correction is simply lacking. Examples include optimisation of electron cooling without electron beam diagnostics, setting up of multi-turn injection in 6 phase-space dimensions and optimisation of longitudinal emittance blow-up with intensity effects. In recent years numerical optimisers, sometimes combined with machine learning techniques, have led to many improvements and successful implementations in some of these areas, from automated alignment of various devices with beam to optimising different parameters in FELs, see for example [1–6].

For a certain class of optimisation problems, the methods of Reinforcement Learning (RL) can bring further advantages. With RL the exploration time that numerical optimisers inevitably need at every deployment is reduced to a minimum - to one iteration in the best case. In 2019 most of the CERN accelerators were in shutdown to be upgraded as part of the LHC Injector Upgrade project [7]. The new linear accelerator LINAC4 and the proton-driven plasma wakefield test facility AWAKE [8] were, however, operated for part

___
* verena.kain@cern.ch

of the year. Taking advantage of recent rapid developments in deep machine learning and RL algorithms, the authors successfully implemented sample-efficient model-free RL for CERN accelerator parameter control and demonstrated its use online for trajectory correction both at the AWAKE facility and at LINAC4. The results were published in [9]. In 2020, trajectory correction with model-based RL could be demonstrated in addition.

This paper is organized as follows. A brief introduction is given to Reinforcement Learning in the domain of accelerator control following [9]. In the experimental section, the problem statements and results of the tests on trajectory correction both for the AWAKE 18 MeV electron beamline and the 160 MeV LINAC4 are given. A short summary of the main outcome of [9] is followed by new results using model-based reinforcement learning. The next steps and potential for wider application are covered in the discussion and conclusion part.

REINFORCEMENT LEARNING FOR ACCELERATOR CONTROL

The optimisation and control of particle accelerators is a sequential decision making problem, which can be solved using RL if meaningful state information is available. In the RL paradigm, Fig. 1, a software Agent interacts with an environment, acquiring the state and deciding actions to move from one state to another, in order to maximise a cumulative reward [10]. The Agent decides which action to take given the current state by following a policy. The goal is to learn the optimal policy for the problem.
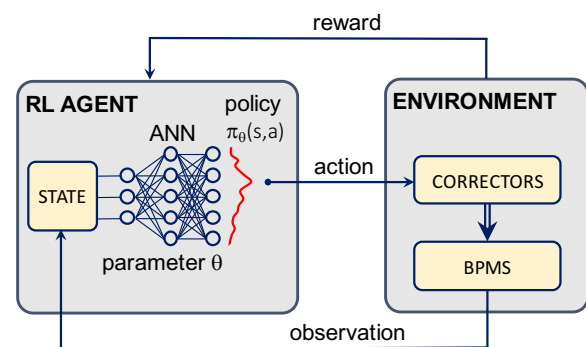

Figure 1: The RL paradigm as applied to particle accelerator control, showing the example of trajectory correction.

Reinforcement Learning algorithms can be divided into two main classes: model-free and model-based. Model-free control assumes no *a priori* model of the environment, learning the system dynamics implicitly from interacting with

MYRRHA-MINERVA INJECTOR STATUS AND COMMISSIONING*

A. Gatera†, J. Belmans, S. Boussa, F. Davin, W. De Cock, V. De Florio, F. Doucet, L. Parez,
F. Pompon, A. Ponton, D. Vandeplassche, E. Verhagen, SCK CEN, Mol, Belgium
F. Bouly, E. Froidefond, A. Plaçais, LPSC, CNRS-IN2P3/UJF/INPG, Grenoble, France
M. Ben Abdillah, C. Joly, L. Perrot , CNRS/IN2P3/IJCLab, Université Paris-Saclay, Orsay, France
H. Podlech, IAP, Goethe-University, Frankfurt a. M., Germany
C. Zhang, GSI Helmholtz Center for Heavy Ion Research, Darmstadt, Germany
J. Tamura, Japan Atomic Energy Agency (JAEA/J-PARC) J-PARC Center, Japan

Abstract

The MYRRHA project [1] at SCK CEN, Belgium, aims at coupling a 600 MeV proton accelerator to a subcritical fission core operating at a thermal power of 60 MW. The nominal proton beam for this ADS has an intensity of 4 mA and is delivered in a quasi-CW mode. MYRRHA's linac is designed to be fault tolerant thanks to redundancy implemented in parallel at low energy and serially in the superconducting linac. Phase 1 of the project, named MINERVA, will realise a 100 MeV, 4 mA superconducting linac with the mission of demonstrating the ADS requirements in terms of reliability and of fault tolerance. As part of the reliability optimisation program the integrated prototyping of the MINERVA injector is ongoing at SCK CEN in Louvain-la-Neuve, Belgium. The injector test stand aims at testing sequentially all the elements composing the front-end of the injector. This contribution will highlight the beam dynamics choices in MINERVA's injector and their impact on ongoing commissioning activities.

INTRODUCTION

The MYRRHA Accelerator is a 600 MeV proton linear accelerator part of a flexible irradiation facility being created by SCK CEN in Belgium as a test-bed for transmutation and as a fast-spectrum facility for material and fuel developments.
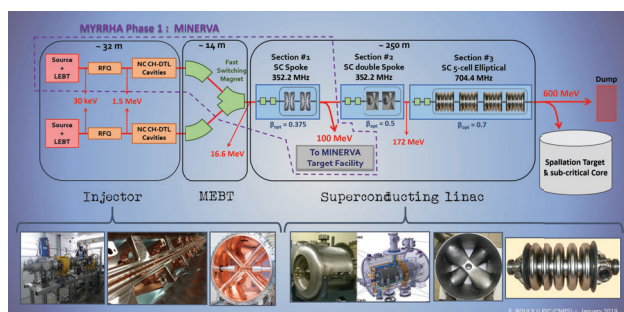

Figure 1: Aceelerator scheme for the 100 MeV (MINERVA) and 600 MeV (MYRRHA ADS) phases [2].

This ADS consists of a low energy section (injector or Linac front-end) characterized by low beam velocity and a highly modular medium-and-high energy section (a so-called main linac) connecting a series of independently controlled accelerating superconducting cavities. Figure 1 depicts the accelerator and its two sections.

When compared with other accelerators of the same class [3], a major distinctive character of this system is given by its considerably harder reliability requirements: in MYRRHA, beam trips of a duration exceeding 3 seconds are considered as a system failure leading to a plant shutdown. In terms of MTBF, this corresponds to requiring a mean time between consecutive failures of at least 250 hours during the system's operative cycle (90 days). A common strategy to meet reliability requirements is given by fault-tolerance, namely the systematic adoption of provisions to compensate for unexpected deviations of the system state originating inside or outside of the system's boundaries. Given the complexity of our linac system, two fault-tolerance design patterns have been selected in function of the characteristics of the section they shall be applied to:

- In the low-energy section, hot spares shall be used as a form of parallel redundancy: two equivalent 16.6 MeV injectors with fast switching capabilities [4] shall be put in place.

- In the main linac section, the availability of similarly structured cavities shall be capitalized so as to realize a serial redundancy strategy, with the functions of failing cavities to be compensated by their four nearest neighbors [5].

The MYRRHA project is scheduled to proceed in stages, with a first accelerator only based on a single injector connected to a superconducting section and an extraction line to a set of target facilities. In the first MYRRHA stage, MINERVA, the main linac shall be based on single-spoke cavities and reach 100 MeV. In a second stage, the accelerator shall be extended with double-spoke and elliptical cavities up to a full-fledged 600 MeV configuration. A final stage will see the accelerator connected to a subcritical nuclear reactor.

THE INJECTOR TEST STAND

The MINERVA injector accelerates the beam up to 16.6 MeV. Its front-end is composed of an ECR proton source, a 2.6 m long LEBT (low energy beam transport line) [6] and a four-rod RFQ accelerating the beam to

---

STUDY ON THE INJECTION BEAM COMMISSIONING AND PAINTING METHOD FOR CSNS/RCS*

Ming-Yang Huang[1,2,3,#], Sheng Wang[1,2,3], Shou-Yan Xu[1,2]
[1]Institute of High Energy Physics, Chinese Academy of Sciences (CAS), Beijing, China
[2]Spallation Neutron Source Science Center (SNSSC), Dongguan, China
[3]University of Chinese Academy of Sciences, Beijing, China

Abstract

In this paper, firstly, the beam commissioning of the injection system for CSNS/RCS will be studied, including: timing adjustment of the injection pulse powers, injection beam parameter matching, calibration of the injection painting bumps, measurement of the painting distribution, injection method adjustment, application of the main stripping foil, optimization of the injection beam loss and radiation dose, etc. Secondly, the painting methods for the CSNS/RCS will be studied, including: the fixed-point injection method, anti-correlated painting method and correlated painting method. The results of the beam commissioning will be compared with the simulation results. Combining with other precise optimizations, the beam power on the target has successfully reached the design value of 100kW and the stable operation of the accelerator has been achieved.

INTRODUCTION

The China Spallation Neutron Source (CSNS) is a high power proton accelerator-based facility [1, 2]. It consists of an 80 MeV H⁻ Linac, a 1.6 GeV rapid cycling synchrotron (RCS), two beam transport lines, a target station, and several instruments. The RCS accumulates the injection beam, accelerates the beam to the design energy of 1.6 GeV and extracts the high energy beam to the target. Its repetition rate is 25 Hz. The design goal of the beam power on the target is 100 kW [3] which had been achieved in Feb. 2020. Figure 1 shows the layout of the CSNS.
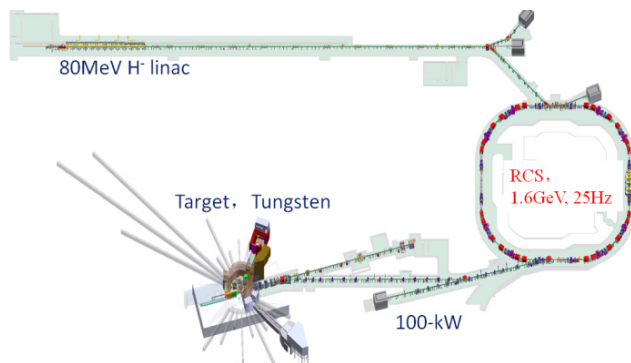

Figure 1: Layout of the CSNS.

Since 2016, the CSNS had begun the accelerator beam commissioning. Figure 2 shows the historical curve of the beam power on the target. It can be seen that: in Nov. 2017, the first 10 kW beam power on the target had been operated for a short while; in Mar. 2018, the beam power over 20 kW had been achieved in the test operation; in Jan. 2019, the beam power was gradually increased to over 50 kW with well controlled beam loss; in Sep. 2019, the beam power in user operation was increased to 80 kW step by step; in Feb. 2020, the beam power was increased to 100 kW to achieve the design goal; in Oct. 2021, the beam power had exceeded 120 kW.
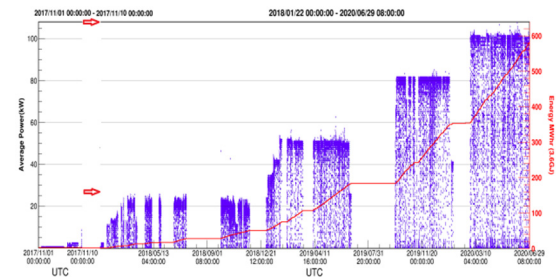

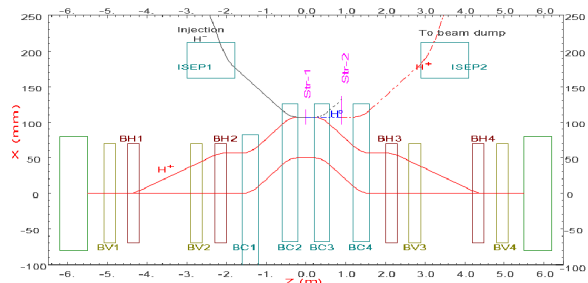Figure 2: Historical curve of the CSNS beam power.

Figure 3: Layout of the CSNS injection system.

The injection system is the core component of the accelerator and the injection beam loss is one of the decisive factors that limit whether the RCS can operate at the high beam power [4]. In order to reduce the beam loss, a combination of the H⁻ stripping and phase space painting method is used to accumulate a high intensity beam in the RCS [5]. Figure 3 shows the layout of the CSNS injection system. There are three kinds of orbit bumps: a horizontal bump generated by four dipole magnets (BH1-BH4) for painting in the horizontal plane; a vertical bump (BV1-BV4) for painting in the vertical plane; a fixed horizontal bump (BC1-BC4) in the middle for an additional closed-orbit shift of 60 mm. There are two carbon stripping foils: a main stripping foil and a secondary stripping foil. Their materials are both HBC.

ACCELERATION OF THE HIGH CURRENT DEUTERON BEAM THROUGH THE IFMIF-EVEDA RFQ: CONFIRMATION OF THE DESIGN BEAM DYNAMICS PERFORMANCES

L. Bellan†, L. Antoniazzi, M. Comunian, E. Fagotti, F. Grespan, M. Montis, , M. Giacchini,
A. Palmieri, M. Poggi, F. Scantamburlo, A. Pisent INFN-LNL, Legnaro, Italy
B. Bolzon, N. Chauvin, J. Marroncle, CEA-IRFU, Gif-sur-Yvette, France
T. Akagi, K. Masuda, K. Kondo, M. Sugimoto, QST, Aomori, Japan
P. Cara, IFMIF/EVEDA Project Team, Aomori, Japan
D. Jimenez-Rey, I.Podadera, CIEMAT, Madrid, Spain
I. Moya, H. Dzitko, C. Yann, F4E, Garching, Germany

Abstract

The Linear IFMIF Prototype Accelerator (LIPAc) is a high intensity D+ linear accelerator; demonstrator of the International Fusion Material Irradiation Facility (IFMIF). In summer 2019 the IFMIF/EVEDA Radio Frequency Quadrupole (RFQ) accelerated its nominal 125 mA deuteron (D+) beam current up to 5 MeV, with >90% transmission for pulses of 1 ms at 1 Hz, reaching its nominal beam dynamics goal. The paper presents the benchmark simulations and measurements performed to characterize the as-built RFQ performances, in the low and high perveance regime. In this framework, the commissioning strategy with a particular focus on the reciprocal effects of the low-medium energy transfers lines and the RFQ is also discussed. In the last part of the paper, the future commissioning outlooks are briefly introduced.

INTRODUCTION

The accelerator setup of LIPAc [1] for the pulse commissioning of the RFQ was composed by the ECR high intensity deuteron ion source [2], the Radio-Frequency Quadrupole [3] and the Medium Energy Transfer Line [4] coupled with a diagnostic plate [5]. The line was terminated with a temporary low power beam dump, with a maximum sustainable DC of 0.1%. First D+ injection was possible in March 2019, then we reached in July 132 kV-2.5 ms-20 Hz and in July 24th we achieved a 125 mA D+ current at 1 ms/1 Hz out the RFQ, with transmission>90%. In order to identify the RFQ performances, it was important to separate the effects on the transmission of the preceding and subsequent parts of the accelerator.

THE RFQ

The Radio Frequency Quadrupole is a 4-vane 9.8 m CW accelerator which accelerates 125 mA positive deuteron beam from 100 keV up to 5 MeV. The maximum Kilpatrick at its nominal file is 1.76. During the RF conditioning at LNL, 1.94 value was reached in the CW regime for 5 hours with the third section of the RFQ. At the state of the art, at the Rokkasho site, in Japan, we reached 1.85 value during pulse conditioning, and we are under high D.C. conditioning of the whole assembly. [6].

---

† luca.bellan@lnl.infn.it

Some design parameters of the RFQ are shown in Fig. 1. The details are reported in reference [7]. However, it is worth re-calling some features that are relevant for this paper:

- The generalized perveance of the nominal beam, from the low energy up to the high section of the accelerator ranges from 10^{-3} to 10^{-5}.
- The tune depression from the shaper is roughly constant, $\frac{\sigma_t}{\sigma_{0,t}} = 0.5$ and $\frac{\sigma_l}{\sigma_{0,l}} = 0.4$
- The input/output beam normalized rms emittance are 0.25/0.26 mm mrad for the transverse plane while the longitudinal rms emittance is 0.2 MeV deg.
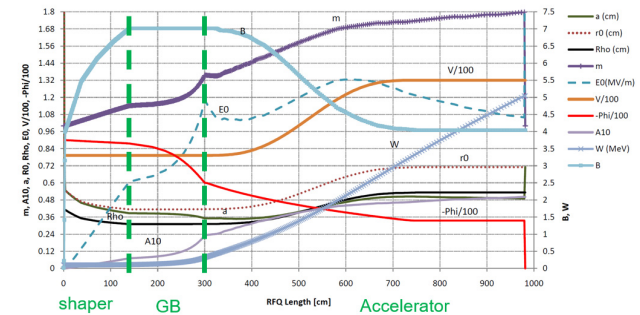

Figure 1: Design parameters of the IFMIF/EVEDA RFQ.

During the Critical Design review, in order to decrease the input beam requirements from the Low Energy Transfer Beam (LEBT) section, easing the beam matching to the RFQ focusing channel, it was decided to decrease the RFQ focusing factor B defined by Eq. (1) smoothly, after the RMS (Radial Matching Section) up to the shaper end, following the undepressed longitudinal phase advance of the RFQ.

$$B = \frac{qV\lambda^2}{mc^2 r_0^2} \qquad (1)$$

The net effect is a drop of the input beam convergence requirements. In particular

- the rms value of the X′ decreases from 43 mrad down to 24 mrad.
- the transmission of the accelerated particles drops form the previous design 95% down to 93.7%.

STATUS OF FRIB COMMISSIONING*

P.N. Ostroumov†, F. Casagrande, K. Fukushima, M. Ikegami, T. Kanemura, S. Kim,
S. Lidia, G. Machicoane, T. Maruta, D. Morris, A.S. Plastun, J. Popielarski,
J. Wei, T. Xu, T. Zhang, Q. Zhao, S. Zhao,
Facility for Rare Isotopes Beams, Michigan State University, East Lansing, MI 48824, USA

Abstract

The Facility for Rare Isotope Beams (FRIB), a major nuclear physics facility for research with fast, stopped, and reaccelerated rare isotope beams, is approaching the commencement of user operation in 2022 as planned. The readiness of the linear accelerator for the production of rare isotopes was verified by the acceleration of Xenon-124 and Krypton-86 heavy ion beams to 212 MeV/u using all 46 cryomodules with 324 superconducting cavities. Several key technologies were successfully developed and implemented for the world's highest energy continuous wave heavy ion beams, such as full-scale cryogenics and superconducting radiofrequency resonator system, stripping heavy ions with a thin liquid lithium film flowing in an ultrahigh vacuum environment, and simultaneous acceleration of multiple-charge-state heavy-ion beams. These technologies are required to achieve ultimate FRIB beam energies beyond 200 MeV/u and beam power up to 400 kW. High intensity pulsed beams capable in delivering 200-kW beams to the target in CW mode were studied in the first segment of the linac.

INTRODUCTION

The FRIB includes a high-power superconducting driver accelerator, an isotope production target, and a fragment separator. The layout of the FRIB is shown in Fig. 1. The FRIB driver linac will provide stable nuclei accelerated to 200 MeV/u for the heaviest uranium ions and higher energies for lighter ions with 400 kW power on the target [1]. The progress with the FRIB linac construction, development, and testing was reported in previous HB workshops, see for example, [2-5]. The 400-kW ion beams will be delivered to a thin fragmentation target which is followed by a large-acceptance high-resolution fragment separator (FS). The FRIB FS will be capable to capture large-emittance rare isotope beams resulting from production reactions, i.e., angular acceptance is ± 40 mrad in both transverse directions and momentum acceptance is ± 5%. The maximum magnetic rigidity of the fragment separator can reach 8 T·m. While many isotopes will be studied in the in-flight experiments, FRIB will use upgraded National Superconducting Cyclotron Laboratory (NSCL) facilities to prepare and re-accelerate stopped isotopes up to 12 MeV/u.

In a continuous wave (CW) superconducting (SC) linac, the 400-kW beams can be achieved with a low beam current, below 1 emA. Therefore, the space charge effects are

mostly negligible in the linac except the ion source and the Low Energy Beam Transport (LEBT). Although the performance of Electron Cyclotron Resonance Ion Sources (ECRIS) has been significantly improved in the past decades, they cannot produce sufficient intensities of the heaviest ions, in order to reach 400 kW on target in a single charge state. To achieve 400 kW power on the target for the heaviest ion beams, multiple charge states of the same ion species are accelerated simultaneously. Particularly, in the case of uranium, two charge states (U^{33+} and U^{34+}) will be accelerated before the stripping and five charge states after the stripping at 17 MeV/u. Also, multiple-charge-state acceleration after the stripper dramatically reduces the total power of unwanted charge states dumped in the first folding segment. Therefore, the multiple-charge-state acceleration will be used for all ion species with a mass above ~60.
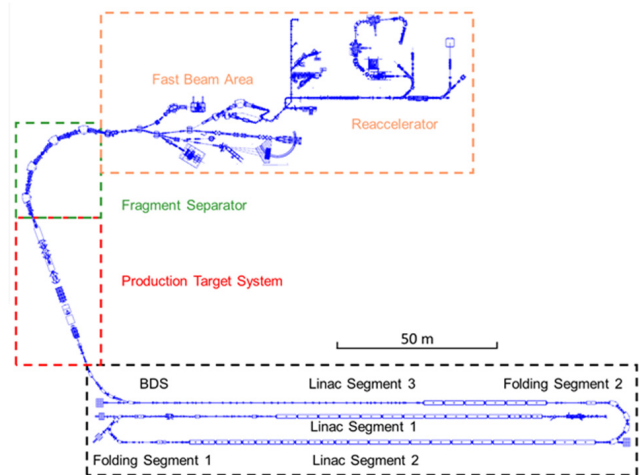

Figure 1: Layout of the FRIB driver accelerator, target, fragment separator, re-accelerator and existing infrastructure. The driver linac consists of three straight segments, Linac Segment 1 (LS1), Linac Segment 2 (LS2), Linac Segment 3 (LS3) and two folding segments, Folding Segment 1 (FS1) and Folding Segment 2 (FS2).

The staged beam commissioning was adopted for the FRIB. The beam commissioning started in 2017 with the Front End (FE) and continued until April 2021. All this time, the installation of the accelerator equipment has been taking place. The current state of the tunnel is shown in Fig. 2. Each stage of the beam commissioning took less than two weeks. The results of each stage were reported in multiple journal papers [6-9]. In this paper, we report the results of the recent commissioning progress. The Kr and Xe beams were accelerated to 212 MeV/u and delivered to

BEAM INSTABILITY ISSUE AND TRANSVERSE FEEDBACK SYSTEM IN THE MR OF J-PARC*

T. Toyama[†1], A. Kobayashi[1], T. Nakamura[1], M. Okada[1], Y. Shobuda[2] and M. Tobiyama[3],
Accelerator division, J-PARC Center, [1]KEK / [2]JAEA, Tokai, Ibaraki, Japan
[3]Accelerator division, KEK, Tsukuba, Ibaraki, Japan

Abstract

In the J-PARC MR, according to the beam power upgrade over 100 kW, beam losses due to transverse collective beam instabilities had started to appear. We had introduced "bunch-by-bunch feedback" system in 2010. Continuing beam power upgrade over 250 kW again caused the transverse instabilities. We introduced "intra-bunch feedback" system in 2014. This has been suppressing those instabilities very effectively. But further beam power upgrade over 500 kW (2.6E+14 ppp, 8 bunches) needs upgrade of "intra-bunch feedback" system. The current understanding of the transverse instabilities in the MR and the effect of the feedback system are presented from the view points of simplified simulation without the space charge effect and measurements. We are upgrading the system in two steps. The first step is "time-interleaved sampling and kicking" with two feedback systems. The second step is getting the sampling rate twice as much as the current rate, ~110 MHz. Details are explained using simulation.

INTRODUCTION

Figure 1 is the layout of the accelerators in J-PARC. The Main Ring (MR) accelerates 8 proton bunches from 3 GeV to 30 GeV [1]. Figure 2 shows beam power history from January 2010 to April 2021. We have two acceleration modes, a slow extraction mode and a fast extraction mode. In the slow extraction mode (Fig. 3, [2]), the beam power is about 64 kW, the beam intensity is 7E+13 protons in a current MR cycling time 5.2 seconds. In the fast extraction mode (Fig. 4), the beam power is about 500 kW, the beam intensity is 2.6E+14 protons in a current MR cycling time 2.48 seconds.
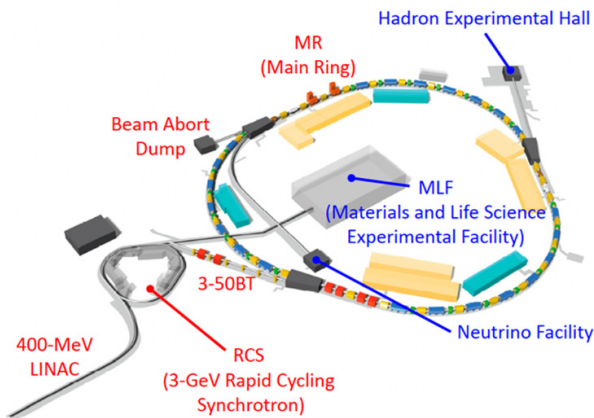

Figure 1: Schematic layout of J-PARC accelerators and experimental facilities.
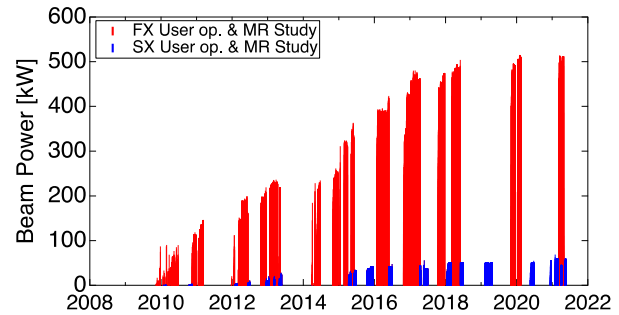
† takeshi.toyama@kek.jp

Figure 2: Beam power history of the MR.
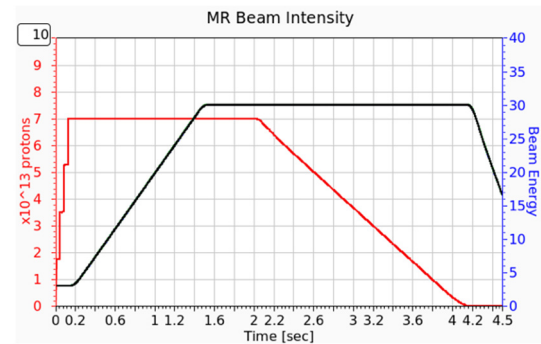
Figure 3: Slow extraction.

Figure 4: Fast extraction.
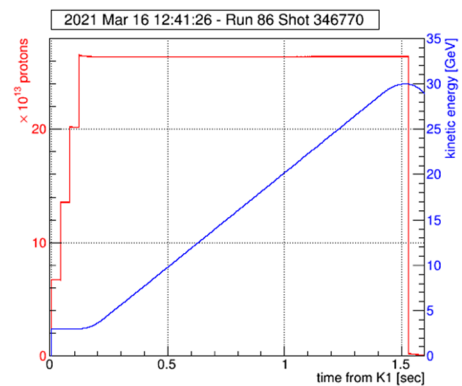
PRESENT OBSERVATIONS IN THE MR

SX Mode

In the SX mode, a bunch-by-bunch feedback system is sufficient to suppress instabilities. Limiting factor to increase the SX beam power is the beam instabilities in debunching process at the 30 GeV flat top [2]. In debunching process at the 30 GeV flat top, longitudinal microwave instability occurs, then electron cloud build-up, transverse

EXPLORING QUASI-INTEGRABLE OPTICS WITH THE IBEX PAUL TRAP

J. A. D. Flowerdew*, S. L. Sheehy, University of Oxford, Oxford, UK
D. J. Kelliher, S. Machida, STFC Rutherford Appleton Laboratory, Oxford, UK

Abstract

An ideal accelerator built from linear components will exhibit bounded and stable particle motion. However, in reality, any imperfections in the magnetic field strength or slight misalignments of components can introduce chaotic and unstable particle motion. All accelerators are prone to these non-linearities but the effects are amplified when studying high intensity particle beams with the presence of space charge effects. This work aims to explore the non-linearities which arise in high intensity particle beams using a scaled experiment called IBEX. The IBEX experiment is a linear Paul trap which allows the transverse dynamics of a collection of trapped particles to be studied. It does this by mimicking the propagation through multiple quadrupole lattice periods whilst remaining stationary in the laboratory frame. IBEX is currently undergoing a nonlinear upgrade with the goal of investigating Quasi-Integrable Optics (QIO), a form of Nonlinear Integrable Optics (NIO), in order to improve our understanding and utilisation of high intensity particle beams.

INTRODUCTION

When designing new particle accelerators, constructing test accelerators can be costly in terms of both financial expense and energy consumption. Once an accelerator is built, it is often difficult to change the lattice structure and thus it is impractical to investigate beam properties over large parameter spaces. Therefore, research and development of accelerator lattices are often performed using simulations. Simulations are a vital part of the accelerator design process, however they struggle to reproduce the intricate physics of the many-body Couloumb interactions (space charge forces) over long timescales (tens of thousands of turns) and can never be a replacement for experimental verification.

These challenges led to the design and construction of linear Paul traps to investigate transverse beam dynamics more efficiently at Hiroshima University, Japan [1], Princeton University, US [2] and, most recently, the Intense Beams Experiment (IBEX), at the Rutherford Appleton Laboratories (RAL), UK [3]. IBEX is a table-top sized experiment that can replicate the transverse betatron motion in alternating gradient accelerators in a dispersion- and chromaticity-free environment.

This paper aims to test a lattice proposed by the theory of Nonlinear Integrable Optics (NIO) by exciting a 4th order resonance and measuring particle loss and phase space evolution. Two different octupole potentials are compared; a normal square wave octupole and an octupole with a strength that scales with the beta function to make the Hamiltonian

time-independent. The time-independent Hamiltonian becomes an invariant of motion and therefore creates a quasi-integrable lattice that should be robust to small perturbations.

THE IBEX PAUL TRAP

The current IBEX trap consists of four stainless steel cylindrical rods and two sets of end caps, each made from four shorter cylinders as seen in the ionisation region of Fig. 1. Argon gas is introduced into the trap via a VAT Series 59 variable leak valve and is ionised with an electron gun. Typically, a sinusoidal RF voltage is applied to the central rods with a maximum peak-to-peak of 300 V and frequency of 1 MHz. Voltages of the same form but opposite polarity are applied to the blue and red outlined rods in Fig. 1 to provide transverse confinement of the ions. A sinusoidal voltage replicates a simple FODO lattice, although it is possible to create more complex lattices in IBEX. Longitudinal confinement of the ions is achieved by applying a DC offset to the end caps.

Adjusting the peak voltage applied to the rods is analogous to changing the quadrupole strength in an accelerator, which in turn changes the betatron tune in both the horizontal and vertical planes. Thus, scanning the rod voltage allows for a wide range of tunes to be scanned over in a short period of time. This is impractical in conventional accelerators and when studying space charge dominated beams over long timescales, it is also impractical to use simulations. Ions can be stored for around 1 s in IBEX, corresponding to 10^6 RF periods. The DC voltage on the end cap is then dropped and the ions are directed onto a Micro-Channel Plate (MCP) or Faraday Cup (FC) detector. The number of ions stored in the trap is controlled by adjusting the length of time that the electron gun is on. This allows for a wide range of intensities to be studied within the trap. Due to the low energy of the ions (< 1 eV), high intensity beam loss studies can be carried out in the trap without damaging or activating components. IBEX has already been used to study coherent and incoherent resonances at high intensities [4].

NONLINEAR UPGRADE TO IBEX

In IBEX's current quadrupolar rod configuration it is only possible to study linear lattice designs. Thus, in order to investigate QIO and NIO, a nonlinear upgrade to IBEX is required. The upgrade will duplicate the linear trap but will also include the addition of four plate electrodes positioned between the rods (shown in Fig. 1 side view). Grounding the four cylindrical rods whilst applying an equal voltage to all four plate electrodes will allow for octupole fields to be realised in the trap. Grounding the four plates while applying voltages of opposite polarity to the red and blue outlined rods will continue to create a quadrupole field. The additional

SLOW EXTRACTION OPERATION AT J-PARC MAIN RING

M. Tomizawa*, Y. Arakaki, T. Kimura, S. Murasugi, R. Muto, K. Okamura,
Y. Sugiyama, E. Yanaoka, M. Yoshii, ACCL, KEK, Tsukuba, Japan,
F. Tamura, JAEA/J-PARC, Tokai, Japan,
H. Nishiguchi, Y. Shirakabe, IPNS, KEK, Tsukuba, Japan,
K. Noguchi, Kyushu University, Fukuoka, Japan

Abstract

A high-intensity proton beam accelerated in the J-PARC main ring (MR) is slowly extracted by using the third integer resonance and delivered to the experimental hall. A critical issue in slow extraction (SX) is a beam loss caused during the extraction. A dynamic bump scheme under an achromatic condition provides extremely high extraction efficiency. We have encountered a beam instability in the de-bunch formation process, which is estimated to be triggered by a longitudinal microstructure of the beam. To suppress this instability, the beam to the MR has been injected into the RF bucket with a phase offset. A newly developed RF manipulation, 2-step voltage debunch, has successfully pushed up the beam power up to 64.6 kW keeping a high extraction efficiency of 99.5%. A drastic beam loss reduction has been demonstrated in the beam test using a diffuser installed upstream of the first electrostatic septum (ESS1). 8 GeV-bunched slow extraction tests for the neutrino-less muon to electron conversion search experiment (COMET Phase-I) have been successfully conducted.
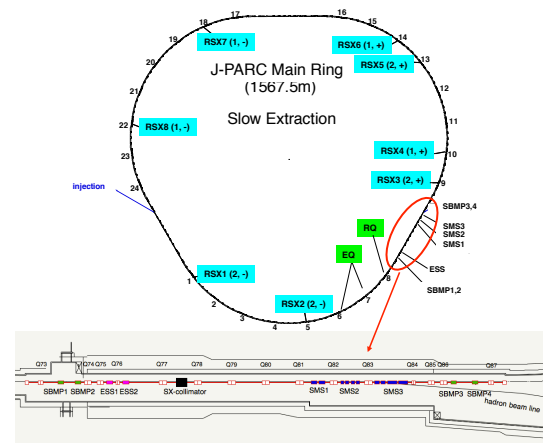
INTRODUCTION

A high-intensity proton beam accelerated in the J-PARC main ring (MR) is slowly extracted by the third integer resonant extraction and provided to the hadron experimental hall to drive various nuclear and particle physics experiments. Most of the proposed experiments are best performed using a coasting beam without an RF structure and a uniform beam intensity during the extraction time.

One of the critical issues in the slow extraction (SX) of a high intensity proton beam is an inevitable beam loss caused at an electrostatic septum (ESS). The slow extraction from the J-PARC MR has unique schemes to reduce the beam loss rate [1]. The first electrostatic septum (ESS1) is located in the section between adjacent focusing quadrupole magnets as shown in Fig. 1. The Courant-Snyder β_x function in this section is ~40 m, which is highest in the MR. In this condition, a large step size (spiral step) Δ at ESS1 can be chosen without causing any primary beam loss in other sections. The head-on hit rate of the beam on the septum in ESS1 can be reduced by the large Δ. The long straight sections in the MR are dispersion-free. If horizontal chromaticity is set to near zero during the extraction, the momentum dependence of the third-integer resonant separatrix can be neglected. When a bump orbit, which moves the circulating beam toward the septum of ESS1, is fixed during extraction,

the outgoing arms from the separatrices can have different angles ($x' = dx/ds$) at ESS1 over the start and the end of extraction (fixed bump scheme). The angles of the bump orbit at ESS1 can be moved to overlap these arms during extraction (dynamic bump scheme). The dynamic bump scheme reduces the side hit rate on the ESS1 septum and reduces the beam losses also at ESS2 and the downstream magnetic septa.

In the actual beam tunings, the transverse septum position of the ESSs and the followed magnetic septa (SMS1 and SMS2) are finely tuned to minimize the beam loss iteratively with the dynamic bump orbit tuning. The beam loss is sensitive to horizontal chromaticity, which is searched to minimize the beam loss rate [1]. We have encountered a transverse beam instability occurring in a debunching process above 30 kW beam power. The mitigations we adopted have played an essential role to rise up the beam power as described in the next section. A current performance of 30 GeV-slow extraction operations, 8 GeV-slow extraction tests COMET Phase-I and future plans toward a higher beam power 30 GeV SX operation are also reported.

Figure 1: Layout of J-PARC slow extraction devices.

BEAM INSTABILITY AND MITIGATIONS

We have encountered a beam loss increase in the slow extraction at the beam powers above 30 GeV. This involves a vacuum pressure rise in the whole ring. An electron cloud has been detected by electron cloud monitors at the debunch formation process [2]. The horizontal and vertical coherent oscillations have been also observed at the same timing. A transverse beam size growth has been observed by a profile

_____
* masahito.tomizawa@kek.jp

COMMISSIONING OF THE ESS FRONT END

N. Milas*, R. Miyamoto, C. S. Derrez, E. M. Donegani, M. Eshraqi, B. Gålnander,
H. Hassanzadegan, E. Laface, Y. Levinsen, M. Muñoz, E. Nilsson, C. Plostinar, A. G. Sosa,
R. Tarkeshian and C. Thomas
European Spallation Source ERIC, Lund, Sweden

Abstract

The European Spallation Source, currently under construction in Lund, Sweden, will be the brightest spallation neutron source in the world, when the proton linac driver achieves the design power of 5 MW at 2 GeV beam energy. Such a high power requires production, efficient acceleration, and transport of a high current proton beam with minimal loss. This implies in a challenging design and beam commissioning of this machine. The linac features a long pulse length of 2.86 ms at a relatively low repetition late of 14 Hz. The ESS ion source and low energy beam transport are in-kind contributions from INFN-LNS. Beam commissioning of this section started in September 2018 and continued until early July in 2019. This article presents highlights from a campaign of beam characterizations and optimizations during this beam commissioning stage.

ION SOURCE AND LEBT OVERVIEW

European Spallation Source (ESS), currently under construction in Lund, Sweden, will be a spallation neutron source driven by a proton linac [1]. The beam commissioning of the ESS linac is being be conducted in stages [2–4]. Commissioning of the first and stage, consisting of the Ion Source (IS) and LEBT, started in September 2018 and continued until early July in 2019. The IS of ESS is a microwave discharge type with the nominal extraction voltage of 75 kV. This type of source is known to produce a high current and high quality beam. As indicated in Table 1, the beam out of the IS includes other ion species, typically around 20% and primarily H_2^+ and H_3^+, which are lost still within the LEBT section. After stable operation was established, the IS provided more than 400 hours of beam time by the end of the beam commissioning period.

Figure 1 is a schematic layout of the LEBT, showing the locations of the two solenoids and other devices. Each solenoid has an integrated pair of dipole correctors (*steerers*) acting on both transverse planes. In between the solenoids, inside the *Permanent Tank,* there are one Faraday Cup (FC), a set o Beam Induced Fluorescence Monitors (BIFMs) [5], and Emittance Measurement Units (EMUs) of Allison scanner type measuring for vertical plane. Beam Current Monitors (BCMs) measure the IS extraction current and also the LEBT output current. The LEBT also houses an iris, which is a movable diaphragm with six blades that mechanically restricts the aperture to adjust the beam current, and a chopper, which adjusts pulse length by deflecting the leading and

* natalia.milas@esss.se

Table 1: ESS IS Possible Operational Parameters

Parameter	Value	Unit
Energy	~75	keV
Peak current (total)	~85	mA
Peak current (proton)	~70	mA
Proton fraction	~80	%
Pulse length	~6	ms
Pulse repetition rate	14	Hz
Duty cycle	~8	%

trailing parts of a pulse. During this first stage of beam commissioning a temporary tank, referred to as *Commissioning Tank*, was placed right after the collimator at the end of the LEBT, providing additional measurement locations closer to the RFQ interface. Inside this *Commissioning Tank* a second EMU (measurement the vertical plane as well) was installed and a second pair of BIFs was available. The use of the BIFMs in a LEBT is a relatively new idea and provided a tool to perform conventional diagnostics techniques, such as an emittance reconstruction based on a gradient scan, even for this part of the linac. Examples of characterizations based on the BIFMs will be presented when discussing the Linear Optics studies in the LEBT.

SOURCE TUNING

In order to tune the IS a scan of 5 parameters is required: the 3 coils confining the magnetic field inside the plasma chamber (referred as Coil 1, 2, and 3, counting from the extraction side), the input RF power for the magnetron and the injected H_2 flux. It was found the source output current was specially sensitive to the Coil 2 strength. Figure 2 shows
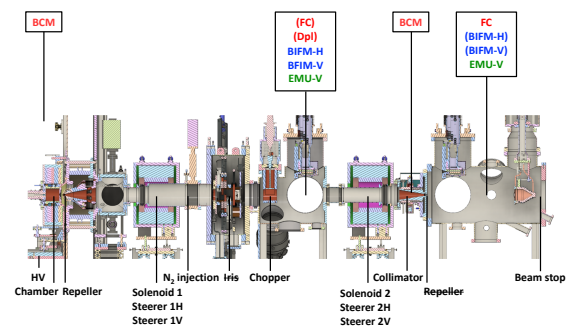

Figure 1: Schematics of the ESS IS and LEBT. a) Close-up of the IS plasma chamber and extraction system. b) IS and LEBT with diagnostics devices.

BEAM ACCELERATION
WITH THE UPGRADED RIKEN HEAVY-ION LINAC

T. Nishi*, M. Fujimaki, N. Fukunishi, H. Imao, O. Kamigaito, T. Nagatomo,
N. Sakamoto, A. Uchiyama, T. Watanabe, Y. Watanabe, K. Yamada
RIKEN Nishina Center, Wako, Japan

Abstract

The performance of the RIKEN heavy-ion linac (RILAC) has been upgraded with a new electron cyclotron resonance ion source and superconducting linac booster (SRILAC). It is expected to have a major role in the synthesis of superheavy elements (SHEs), development of the technologies for production of medical radioisotopes, and as a powerful injector to the RI Beam Factory. Here, we report on the beam delivery for the SHE experiment that began in June 2020, particularly on the adjustment of the optics based on the measured phase ellipse.

INTRODUCTION

The RIKEN Nishina Center has been conducting experiments to search for new superheavy elements using RIKEN heavy-ion linac (RILAC) [1]. Recently, a new 28-GHz electron cyclotron resonance (ECR) ion source [2] and superconducting linear accelerator (SRILAC) [3] were constructed to increase the beam intensity and beam energy. The low-energy beam-transport (LEBT) system is equipped with slit triplets that control the beam emittance in the RILAC. The beam energy and beam positions are measured using eight sets of capacitive pickups called BEPM (beam energy position monitor) installed in the cold section of the SRI-LAC [4, 5].

In January 2020, we obtained the first beam from SRILAC. The Ar^{11+} with an intensity of $2\,p\mu A$ was accelerated up to 5 MeV/u [6]. From July 2020, we began to deliver the high-intensity V^{13+} beam with energy of 6 MeV/u to the GARIS-III [7] experiment. To transport the high-intensity heavy ion beam to the GARIS-III target with acceptable beam loss, we have established a method of measuring the phase ellipse and adjusting the optics based on the measured phase ellipse and optical simulation. This method enables us to optimize the optics flexibly according to the beam state, which varies depending on the ion source and slit conditions, as well as the experimental requirements.

HIGH ENERGY BEAM TRANSPORT LINE

The heavy ion beam, accelerated to approximately 6 MeV/u in the SRILAC, passes through a differential pumping system [8] and is then transported to GARIS-III through a beam transport called the high-energy beam transfer (HEBT) line (Fig. 1). The inner diameter of this beam transport is 62 mm, and its configuration is TQ - TQ - D - SQ - SQ - DQ (TQ = triplet quadrupole, D = dipole, SQ = singlet quadrupole, DQ = doublet quadrupole). D is a 90° bending
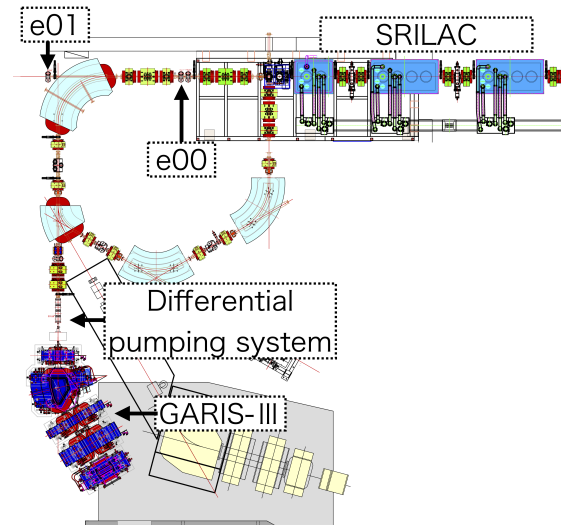
_____
* takahiro.nishi@riken.jp

Figure 1: Top view of SRILAC, high-energy beam transfer line, and GARIS-III. A middle point denoted as e00 is considered the object point for optical calculation.

magnet with edges cut at 25° at both ends. Additionally, a bending magnet is placed between SQ and DQ, but it is not excited during the beam transport to GARIS-III. GARIS-III is filled with He gas at $\simeq 70\,Pa$ during the experiment, while the vacuum of the HEBT line must be maintained at 10^{-5}–$10^{-6}\,Pa$. Therefore, the inner diameter of the beam pipe immediately before the target is narrowed to $\phi 25\text{-}15\,mm$, and the gas is continuously evacuated by a vacuum pump. The requirements for the beam transport of the HEBT line are (A) a beam loss less than a few percent and (B) the adjustability of beam spot shape on the GARIS-III target depending on the experimental conditions. The first requirement is particularly important for maintaining for the radiation safety. Since the side wall of GARIS-III is relatively thin, it is necessary to measure and confirm the radiation while optimizing the beam transport. For the second requirement, a horizontally flatted ellipse is desired in the production run to prevent local depletion of the rotating target, while a large circle shape is desired in the calibration run. To satisfy these requirements, the beam envelope should be narrower immediately before the target, where the acceptance is relatively smaller and wider at the target.

PHASE ELLIPSE MEASUREMENT AND OPTICS TUNING

In the operations of the upgraded RILAC, the optical system was adjusted in two steps. First, phase ellipse of the beam at e00, defined as the object point in the optical